

13

ISRIC LIBRARY
CR
1994.07
Vrije Universiteit, The Netherlands

FORMATION OF SURFACE COATINGS ON VOLCANIC EJECTA AT FOUR VOLCANOES IN COSTA RICA

(15g8)

karin groenesteijn
(J050-711)

<1994>
publ. 97-005



examiner
prof. N. van Breemen

supervisors
toine jongmans
peter buurman
jan mulder

Scanned from original by ISRIC – World Soil Information, as ICSU World Data Centre for Soils. The purpose is to make a safe depository for endangered documents and to make the accrued information available for consultation, following Fair Use Guidelines. Every effort is taken to respect Copyright of the materials within the archives where the identification of the Copyright holder is clear and, where feasible, to contact the originators. For questions please contact soil.isric@wur.nl indicating the item reference number concerned.

15N 30039

The picture on the cover shows an eroded coating at the surface of layered ash deposits at the Poás.

PREFACE

This report is the written result of a 840 sbu thesis I have done in the field of soil formation and ecopedology at the department of soil science and geology, Wageningen Agricultural University. Weathering of primary and formation of secondary material can be considered as the first steps towards the formation of soils. To study these processes recently active volcanoes are highly suitable, as they offer high amounts of easily weatherable primary material. This study involves the formation of coatings at four volcanoes in Costa Rica. Included were a period of field work in Costa Rica and a period of analysing and interpreting in Wageningen. The field work was essential in order to form a mental picture of the processes that are taking place at the volcanoes. Only when you see and hear the eruptions, feel the ash raining down, taste the acid precipitation and smell the sulfur you can imagine the pace at which the weathering takes place.

Besides the interesting nature of the subject itself, this thesis offered the possibility to get acquainted with various optical techniques. The combination of these optical techniques with chemical analyses was a fascinating one. The chemistry has served to support the optical observations. Yet the chemistry became more and more fascinating and I would have liked to study it for some more time. I realize that a lot more can be done with the chemical results that were gathered. Unfortunately the chemical labwork took more time than planned, resulting in a short time left for interpretation of the chemical results.

I would like to thank Toine Jongmans for his inspiring way of supervising and his great enthusiasm. I would like to thank Peter Buurman and Jan Mulder for their supervising of the chemical part of this study, and André Nieuwenhuyse for his chauffering and company during the field work in Costa Rica. Finally I would like to thank the Dr. Hendrik Muller's Vaderlandsch Fonds and the Wageningen Fonds for their financial support, which enabled the field work in Costa Rica.

CONTENTS

	page no
1 INTRODUCTION	1
2 MATERIALS AND METHODS	2
2.1 Geology and study sites	2
2.1.1 <i>The Arenal</i>	2
2.1.2 <i>The Turrialba</i>	3
2.1.3 <i>The Poás</i>	3
2.1.4 <i>The Rincón de la Vieja</i>	3
2.1.5 <i>Drainage conditions</i>	4
2.1.6 <i>Parent material</i>	4
2.1.7 <i>Acid environment</i>	5
2.2 Field sampling	5
2.3 Analysis	5
2.3.1 <i>Optical methods</i>	5
2.3.2 <i>Microchemical and mineralogical analysis</i>	6
2.3.3 <i>Analysis at fractionated volcanic ash</i>	6
2.3.4 <i>Water analysis</i>	7
2.4 Weathering experiment	7
3 OPTICAL OBSERVATIONS AND INTERPRETATION	9
3.1 Detailed field description	9
3.2 Optical observations	10
3.2.1 <i>Binocular observations of coatings</i>	10
3.2.2 <i>Micromorphology on thin sections of coatings</i>	10
3.2.3 <i>Submicroscopy</i>	13
4 CHEMICAL RESULTS AND INTERPRETATION	
4.1 Chemistry of solid material	19
4.1.1 <i>XRF analysis</i>	19
4.1.2 <i>Guinier diffraction pattern</i>	19
4.2 Chemistry of solutions	19
4.2.1 <i>Field water sample analysis</i>	19
4.2.2 <i>Analysis solutions weathering experiment</i>	21

4.3	Neoformation	23
4.3.1	<i>Allophane and imogolite</i>	23
4.3.2	<i>Gibbsite</i>	24
4.3.3	<i>Kaolinite</i>	24
4.3.4	<i>Amorphous silica and aluminum</i>	25
4.4	Interpretation	25
4.5	Coating genesis	26
	REFERENCES	27

1 INTRODUCTION

Weathering of primary- and formation of secondary minerals are dominant soil forming processes in materials that contain appreciable amounts of easily weatherable minerals (Jongmans, 1994; Nahon, 1992; Delvigne, 1965).

Factors influencing the rate of weathering are climate, parent material, vegetation, drainage and age. Humid conditions, high temperatures and easily weatherable parent material like andesitic volcanic ejecta favour rapid weathering (Nieuwenhuyse et al., 1994). Under such conditions basic cations are leached, and more Al and Si may be liberated than crystalline neoformed material can be formed. (Shoji et al. 1993). Such conditions favour the formation of amorphous materials like opaline silica, allophane and imogolite (Wada, 1989). Especially under an isohyperthermic temperature- and a perodic moisture regime (Soil Survey Staff, 1992) amorphous materials occur frequently. Such regimes are present in the volcanic mountainous area in the central part of Costa Rica.

On the slopes of active volcanoes in this region high weathering rates can be expected, due to the abundance of easily weatherable minerals in andesitic volcanic ejecta, high precipitation and the acid conditions that are usually found in the direct environment of volcanoes with fumarolic activity (Alfaro, 1988). The elements liberated during weathering will partly be leached, especially those that are highly soluble. Some elements will form secondary materials, especially in large voids in the upper soil horizons or at the soil surface, where the soil solution easily can be oversaturated as a result of rapid evaporation. We observed hard, thin coatings on ^{andesitic} scoria and rockfragments situated on the slopes of four different volcanoes in central Costa Rica.

The goal of this study is to characterize the morphology of the surface coatings and to derive a concept for their formation. To our knowledge no other studies have been carried out before with respect to this topic.

Different techniques are used to characterize the coatings in the field and at microscopic and submicroscopic level. (Micro)morphological techniques alone are insufficient to determine the chemical and mineralogical composition of the coatings. The relation between optical and chemical properties is in theory clear, in practice it is not always easy to examine. Microfeatures observed with optical methods are often too small to prepare for common chemical analysis. However, the Scanning Electron Microscope with Energy Dispersive X-Ray Analyzer (SEM-EDXRA, e.g. Bisdom et al., 1990) can give a semi-quantitative analysis of the chemical composition of very small phenomena, observed in uncovered thin sections.

The soil solution that comes into contact with the primary material largely controls the composition of neoformed material. To relate the optically determined concept of coating formation to the actual chemical field conditions, water was sampled at the volcanoes and chemically analysed.

In addition a weathering experiment was done with fresh volcanic material to imitate the cyclic process of wetting, weathering, precipitation due to evaporation, drainage and rewetting that is likely to occur at the volcanoes. The solutions obtained in this experiment were analysed and compared with the water samples from the field. The chemical data are finally linked to the concept of coating formation. Based on this linkage we gather a final conclusion.

and the Pacific Ocean. The country is bounded to the north by Nicaragua and to the south by Panama. The two oceans are separated by the Central Cordillera, which is the backbone of the country. The Central Cordillera is a range of mountains that runs roughly north-south through the center of the country. It is composed of several smaller mountain ranges, including the Guanacaste Range, the Cordillera Volcanica Central, and the Talamanca Range. The Central Cordillera is the site of many active volcanoes, including Poas, Barva, Irazu, and Turrialba.

The Pacific Ocean is to the west of the Central Cordillera, and the Atlantic Ocean is to the east. The country is divided into several provinces, including Alajuela, San Jose, Cartago, Heredia, San Carlos, and Limon. The capital city, San Jose, is located in the central part of the country, near the Pacific Ocean.



Figure 1. Map of Costa Rica, showing the locations of volcanoes. Historically active volcanoes are indicated with an asterisk. (US Geological Survey, s.a.)

2 MATERIALS AND METHODS

2.1 Geology and study sites

Four volcanoes were selected for this study. They are all part of the volcanic range in central Costa Rica that runs from the northeast to the southwest, parallel to the pacific coast. This mountain range is formed due to subduction of the oceanic Cocos Plate under the continental Caribbean plate (Weyl, 19..). With increasing pressure and temperature, the oceanic plate material melts. The magma and gases formed, are lighter in weight than the solid surrounding. As a result of this they are pushed upwards to the earth surface and find their way out in the form of volcanoes.

2.1.1 *The Arenal*

The Arenal is a conically shaped stratovolcano, in the northwest of Costa Rica (see figure 1). It covers an area of 33 km^2 and has an height of 1633 m a.s.l. the current eruption activity starts in 1968. The Arenal is constituted of alternate layers of volcanic ash and angular lapilli, blocky lava flows and deposits of blocks from glowing avalanches. In 1993 a thick layer of ash was deposited in the surroundings of the volcano.

The present activity consists of explosions of low intensity throwing up ashes, rocks, gases and steam, usually with intervals of 5 to 200 minutes.

The size of the ash is dominantly smaller than 2 mm. It is mainly deposited at the west flank of the volcano.

The rock fragments thrown out, form blocky lava flows which may reach a length of a few km's. The lava flows cover almost one third of the slopes of the volcano.

The samples were all taken at the west flank of the volcano at an altitude of 700 to 750 m a.s.l. The mean angle of the slope is about 20° . The material found on this slope consists mainly of deposits from the pyroclastic avalanches from the explosive eruptions from 1968. During this eruption large blocks were thrown out which produced impact craters with a depth up to 4 metres. (Alvarado, 1993). The large blocks are now situated at the surface. These observations indicate the high grade of erosion that takes place, mainly as a result of the enormous amounts of rain water that rapidly run off the slopes at showers, not hindered by a closed vegetation. The gullies that incise the surface are not able to drain all this water, so periodically a highly erosive runoff water layer of 5 to 10 cm covers the whole slope.

At the same time a continuous supply of fresh andesitic ash takes place. The system can therefore be described as being dynamic.

The vegetation at the western slope is very open. Most of the vegetation is found on the lava flows. Here the stage of development of the vegetation, mainly mosses and grass, is an indication of the age of the lava flow.

The erosive slopes are scarcely vegetated with moss and low bushes.

The mean yearly temperature at the sampling site should be approximately 23°C , with a difference of about 2° between the coldest and warmest month (Herrera, 1985). Precipitation is high, though no exact figures are known (perudic moisture system).

The precipitation can be increased because the air is forced upwards at the eastern side of the volcano and thus may contain more water vapour. In addition, the fine ash particles thrown into the air can act as condensation nuclei.

2.1.2 *The Turrialba*

The Turrialba (approx. 3340 m a.s.l.) is a stratovolcano which shares its base with the Irazú volcano (twin volcanoes). The massif covers an area of 500 km². The upper structure of the Turrialba is conic, it possesses three well-defined craters of which the central and deepest crater is approximately 50 m in depth.

The last recorded eruptive activity has been around 1865. At present the craters have exhalative activity with emission of various gases and steam with deposits of native sulphur. Temperatures of the fumaroles vary between 85° and 88°C in the central crater. The mean annual temperature at this altitude is 8° Celsius, with a difference of 4° between the warmest and coldest month. However the temperature of the surface in the central crater is much higher because of the geothermal activity. (Herrera, 1985)

The annual precipitation is about 2040 mm, with a minimum of 30 mm in march and a maximum of 280 mm in November (Hartman, 1992). Vegetation is absent near the fumaroles, at more distance mosses and low bushes are found.

Samples were taken in the central crater; near the fumaroles (within 25 m). According to the pure sulfur deposits that we found near the fumaroles, much sulfur is emitted, and the environment will be very acid.

Study from

2.1.3 *The Poás*

The Poás (2708 m a.s.l.) is a complex stratovolcano, which covers an area of 300 km². On the summit different cones and craters are present. The main crater is circular shaped with a diameter of 1300 m and a depth of 300 m. Four principal morphogenetic units can be distinguished: the eastern plateau (pelón), the crateral lagoon, the lava dome and the inside beach. The crater lake present in the crateral lagoon has a pH of practically zero, and is thereby the world's most acid natural lake. The Poás has been quite regularly active for at least the last two centuries. At present the activity is mainly fumarolic (escaping of hot gases and steam). (Alvarado, 1993) Emissions from the fumaroles and the phreatic eruptions form large white or yellowish gas plumes which are spread by the wind. The environment is strongly acidified by the dry and wet deposition of these gases and their reaction products. (see par. 2.1.7) The mean annual temperature is about 13° Celsius, with a difference of 4 degrees between the warmest and coldest month (Herrera, 1985). The vegetation, if present, consists mainly of mosses.

Samples were taken at the slope in the crater and at the eastern plateau ('cerro pelón'). This plateau is situated downwind from the active area and therefore receives a great amount of acidity. Alfaro et al. (1986) reported mean pH's of 2.98 for the wet deposition at this plateau.

2.1.4 *The Rincón de la Vieja*

The Rincón de la Vieja volcanic massif is located in the northwest of Costa Rica. Its summit is an elongated ridge composed of at least 9 eruptive vents clustered together. The maximum altitude of this volcano is 1895 m a.s.l.; and the complex covers more than 400 km². The Rincón de la Vieja has been rather active in the last 140 years; the last eruptions have been reported in 1985, 1987 and 1991. At present the volcano shows fumarolic activity.

The mean annual temperature at the sampling sites is about 18° Celsius, with a difference of 4° between the warmest and coldest month. (Herrera, 1985)

Samples were taken at the western slope at 1500 m a.s.l. and at the rim of the crater (about 1700 m a.s.l.) which is the most active at present. The slope consists mainly of rather coarse scoria. The sampling site at the slope has a mean angle of about 30°. The vegetation is very open, and absent higher at the volcano.

2.1.5 *Drainage conditions*

As mentioned before, most of the precipitation is drained superficially. However, water will be retained in the (micro)pores in the layered, alternately textured material of the uncovered slopes and at rock surfaces. This water will start to evaporate quickly as the rain has stopped as a result of the high input of solar radiation at the bare surface.

If high temperatures are reached at the surface, for instance at the Turrialba, this will increase the evaporation at the surface. Water that infiltrates in scoria and ash will probably partly reach the atmosphere again as steam from the fumaroles.

2.1.6 *Parent material*

The mineralogical composition of the lava's is andesitic to basaltic-andesitic. The lava contains large amounts of volcanic glass that ranges in colour from colourless to violet and can contain microcrysts of minerals. The composition of the phenocrysts (which forms 24 to 60 % of the material) is given in table 1.

Table 1. Composition of phenocrysts in the lava of the Arenal (Alvarado, 1993).

mineral	weight%		
plagioclase (An 44-89)	17.5	-	48
augite	0.5	-	13.5
hypersthene	0.5	-	7.5
olivine	0	-	5
magnetite	0.5	-	1.7
apatite	0.5	-	1

opname The relative stability of the components of the volcanic ash is as follows (Aomine and Wada, 1962; Loughnan, 1969; Mitchell, 1975; Shoji et al., 1974; Yamada et al., 1978; Shoji et al., 1993) :

Coloured volcanic glass < noncoloured glass = olivine < plagioclase < augite < hypersthene < hornblende < ferromagnetic minerals

Olivine is considered to be as susceptible to chemical weathering as noncoloured volcanic glass; however, it occurs only in small amounts in volcanic ash. The plagioclase minerals are highly weatherable among the crystalline primary minerals, with those of calcic composition being more susceptible to weathering than those of sodic composition. (Shoji et al., 1993)

2.1.7 Acid environment

The principal volcanic gases of the Arenal and Poás that can transform into acids on the soil surface are CO₂, H₂S, HF and SO₂, where SO₂ is the major compound of volcanic gases (Malavassi et al, 1984; Alfaro, 1988). It is estimated that the fumaroles of the Poás produce hundreds of tons of sulphur dioxide daily. The Arenal sends into the air approximately two hundred tons of sulphur dioxide per day. (Cheminee et al., 1981; Alfaro, 1988). Alfaro et al. (1988) reported that the pH of dry deposition ranged between 3.5 to 4.5 in their study area at the Arenal volcano. At the Poás the lowest pH found was 2.4 and the highest 6.0. Especially the downwind areas receive acidity with dry and wet deposition. Although such data are absent for the Rincón de la Vieja and Turrialba we assume that a similar situation exists at these volcanoes.

2.2 Field sampling

At all the volcanoes studied, hard, thin coatings occur on surfaces of unconsolidated ash/scoria deposits and on surfaces of rock fragments. The sample sites were described in detail and samples were taken of surface coatings including underlying ash/scoria deposits and rocks. These samples were used for preparation of thin sections and additional submicroscopical observations.

Difficulties arose in collecting fresh, unweathered ash to perform a weathering experiment. The Arenal is the only volcano that currently throws up fresh ash. We tried to catch it using a piece of plastic of 2 by 2 metres. It was impossible to collect enough material this way because of the frequency of showers that wash the material away. Therefore we added fresh ash collected from the soil surface.

Water samples were taken to determine the composition of the soil solutions involved. Precipitation was collected with funnels. Water, running off rocks, was collected with the aid of a gutter, mounted at one side at the rock fragment. With rhizon-samplers and vacuum bottles with septum, water was sampled under coatings, out of moss covering soil surfaces and rock fragments, and from puddles where it had collected. Water samples, not collected with a rhizon-sampler were afterwards siphoned with a rhizon to filter out fine material possibly caught in. To study the effect of not filtering, one sample of precipitation with fine ash included, was divided in two parts of which one was filtered and the other not. The water samples were stored in a refrigerator at 4° C when possible.

2.3 Analysis

2.3.1 Optical methods

The coating surfaces and vertical cross sections of coatings and underlying material were examined and described with the use of a Leitz binocular. This binocular is an excellent instrument to bridge the gap between field- and petrographic microscope observations.

Before impregnation of the undisturbed samples for thin section, the water was replaced by acetone according to the method of Miedema et al. (1974). Afterwards they were impregnated with polyester raisin. Thin sections (5 by 3 cm) were prepared following the method of Fitzpatrick (1970), and examined with a petrographic light

microscope in plane polarized, and crossed polarized light. Micromorphological features were described following the terminology of Bullock et al. (1985).

The scanning electron microscope (SEM-EDXRA) was used to study coatings in uncovered thin sections, rough coating surfaces and vertical cross sections of coatings with high magnifications. Photographs were made of the characteristic phenomena.

2.3.2 Microchemical and mineralogical analysis

In situ semi quantitative microchemical analysis using SEM-EDXRA (Philips, Eindhoven, the Netherlands) was performed on uncovered thin sections, coating surfaces and a cross section of a coating. The peaks of the EDXRA signals were linearly transformed to element-masspercentages by comparison with standard minerals.

With the Guinier-camera an X-ray diffraction pattern was obtained of coating material isolated with a small dentist drill.

2.3.3 Analyses at fractionated volcanic ash

The grain size distribution of the Arenal ash was determined with the an LS particle size analyser (Coulter Electronics, Mijdrecht, the Netherlands). The median of the ash was 359.0 μm . Figure 2 gives the particle size distribution of the ash.

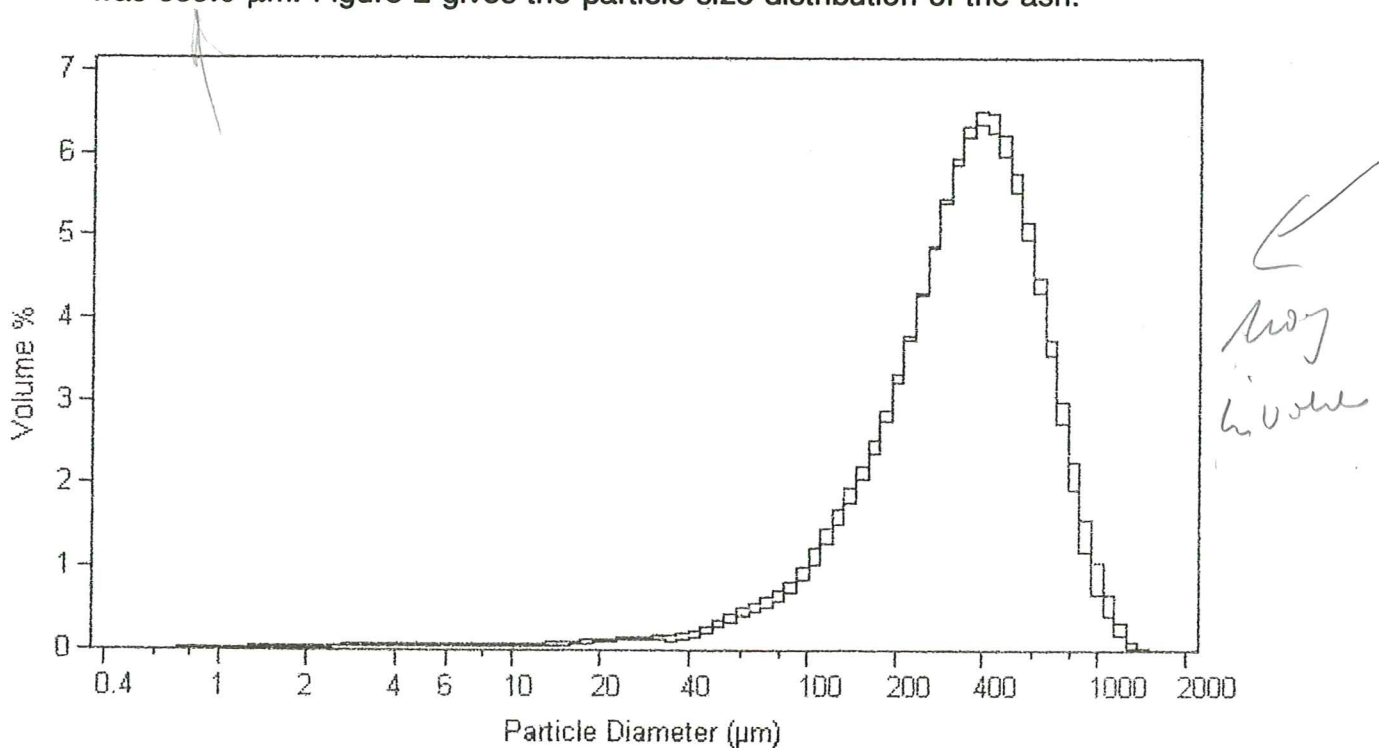


Figure 2. Particle size distribution of the Arenal volcanic ash.

The unweathered ash was dried and separated in five fractions (see table 2). These fractions and the bulk sample were used in the weathering experiment.

Table 2. Particle size of separated ash fractions used in the weathering experiment.

fraction	particle size in μm	
I	< 53	<i>March 8/4</i>
II	53 - 105	
III	105 - 212	
IV	212 - 500	
V	> 500	
bulk	not fractionated	

A total analysis of major and minor elements was done in the different fractions by X-Ray fluorescence on $\text{Li}_2\text{B}_4\text{O}_7$ glass disks and presented as mass fractions of oxide components. The XRF system was calibrated using the USGS geochemical standards as listed by Abbey (1980).

2.3.4 Water analysis

The chemistry of the water samples and the solutions of the weathering experiment was analysed using the methods described in the Manual for Chemical Water Analyses by Velthorst (1993). The samples taken in the field were analysed by the lab personnel, the solutions obtained with the weathering experiment were done by myself. Sodium, potassium, calcium, iron and magnesium were analysed with the AAS; silica and aluminum were analysed using the auto-analyser. Chloride, nitrate and sulphate of the samples taken in the field were analysed with the HPLC. (Velthorst, 1993)

2.4 Weathering experiment

The material at the volcanoes is wetted and rewetted with acid precipitation. To study the processes that take place due to this mechanism, a weathering experiment is performed with acid solution. From each of the separated grain size fraction of the volcanic ash of the Arenal (see par. 2.3.3) and the bulk sample 2.50 g was used for the weathering experiment. The samples were mechanically shaken with 50.0 ml of a 10^{-3} M hydrochloric acid solution (pH 3.0). After 2 days the suspensions were centrifuged and the solution was poured off. This was repeated five times with the same solid material.

Simultaneously a similar weathering experiment was done with distilled water to study the influence of high concentrations of acid at the weathering. Of the same ash samples 4.00 g was weighed in and shaken for 7 days with 80.0 ml of distilled water.

The pH of the solutions obtained was measured directly with an Orion Research pH meter with combination pH electrode. After that, the solutions were filtered with 0.2 μm microfilters and stored at a temperature of 4°C. The solutions were analysed in the

same way as the water samples taken in the field. Chloride, nitrate and sulphate were not analysed in the solutions from the weathering experiment with acid water, due to mechanical problems with the HPLC.

The concentrations and ratios found in the experiment were compared with those found in the samples taken in the field. With the obtained data equilibria were calculated with respect to the formation of secondary minerals.

3 OPTICAL OBSERVATIONS AND INTERPRETATION

3.1 Detailed field description

The coatings studied are hard, frequently layered, thin crusts with a rather light greyish colour. They occur at the surface of unconsolidated volcanic ash as well as at horizontal and vertical surfaces of rock fragments exposed to the air. Large parts of the soil surface can be covered and cemented by these coatings. Dead trees and root surfaces exposed to the air are also partially covered by coatings, suggesting that in situ weathering of material directly underlying the coating is at least not the only factor concerned in coating genesis.

At the soil surface, there is a strong relation between coating relief and the texture of the volcanic ash. Coatings with smooth relief occur at fine textured material whereas at coatings with high surface relief occur at coarser textured material.

The coatings on the unconsolidated ash deposits seem to be situated mainly at places that are less dynamic. At more dynamic places coatings are being eroded physically; the coatings show cracks and fall apart in platy pieces that are washed away.

In very fine material coatings were observed near to moss pillows. The moss pillows consist of a densely packed mixture of fine green, living organic material and very fine textured volcanic ash. Apparently the moss pillows act as collectors of very fine ash, probably because they are continuously moist.

There seems to be an interaction between the occurrence of the coatings at these sites and the moss. The moss pillows partially overgrow the coatings at the sides. Under the centre of the moss pillows coatings are absent. At the same time, coatings can occur on top of dead moss packs covered with a layer of very fine ash.

 The coatings found at rock surfaces are fairly similar to the coatings developed at the soil surface, except for the coating relief, which is more roughly developed. Small depressions in the rock fragments are partly filled in by volcanic ash. On top of this unconsolidated ash new (thin) coatings can develop. However, due to their friable consistency, these thin coatings are very susceptible to erosion. This is probably the origin of the remnant fragments of coatings present along the sides of such small depressions. Similar coating fragments are observed at the side and bottom of rock fragments. We suppose this to be remnants of coatings that continued from the rock fragment at the soil surface. A few of these coating remnants can be found above or next to each other, indicating the alternation of coating formation and erosion.

 The boundary between rock fragment and soil surface is frequently undistinguishable, because coatings continue seamlessly from rock to soil surface. This observation indicates that coatings at the soil surface and rock fragments are similar and have the same genesis.

The coatings at the four volcanoes show small differences in appearance. At the Turrialba, coatings found in vertical position at the wall of a gully. These coatings have a very irregular surface, with distinct protruding pendants in horizontal direction. These pendants can be up to 2 cm thick. The occurrence of pendants is an indication for growth of the coating from solutions.

At the plateau at the Poás almost the entire surface consists of coatings, which have developed on different layers of ash. The surface is subjected to strong physical

erosion. The ash layers still covered with coatings form table mountains at meso-scale (see picture on cover).

At the rim of the crater of the Rincón de la Vieja are found very thick coatings (up to 8 mm) with distinct layers, which continue in pendants. These coatings nearer to the crater are thicker than coatings at the slope.

Gypsum crystals were observed at the slope of the Arenal. This accentuates the acid environment, as a considerable amount of SO₄ is needed to form gypsum.

3.2 Optical observations

3.2.1 *Binocular observations of coatings*

The coatings present on the unconsolidated ash deposits and rock fragments at the Arenal show a rather translucent, fine textured groundmass with very fine granular material floating in it. The coating surface has a wavy appearance. The high parts contain little incorporated granular material, whereas the lower parts contain appreciable amounts of mineral particles and are consequently less translucent and lighter coloured. Vertical cross sections reveal the laminated character of the coatings. Layers of fine textured material with minor amounts of mineral grains are alternated with layers dominantly consisting of fine mineral particles and little of the fine textured material, suggesting that neoformation and deposition of fine mineral grains occurs simultaneously.

The coatings found at the Poás have a smooth surface with cracks in it. The material is less translucent and consist of very thin layers. There are few contaminations in it.

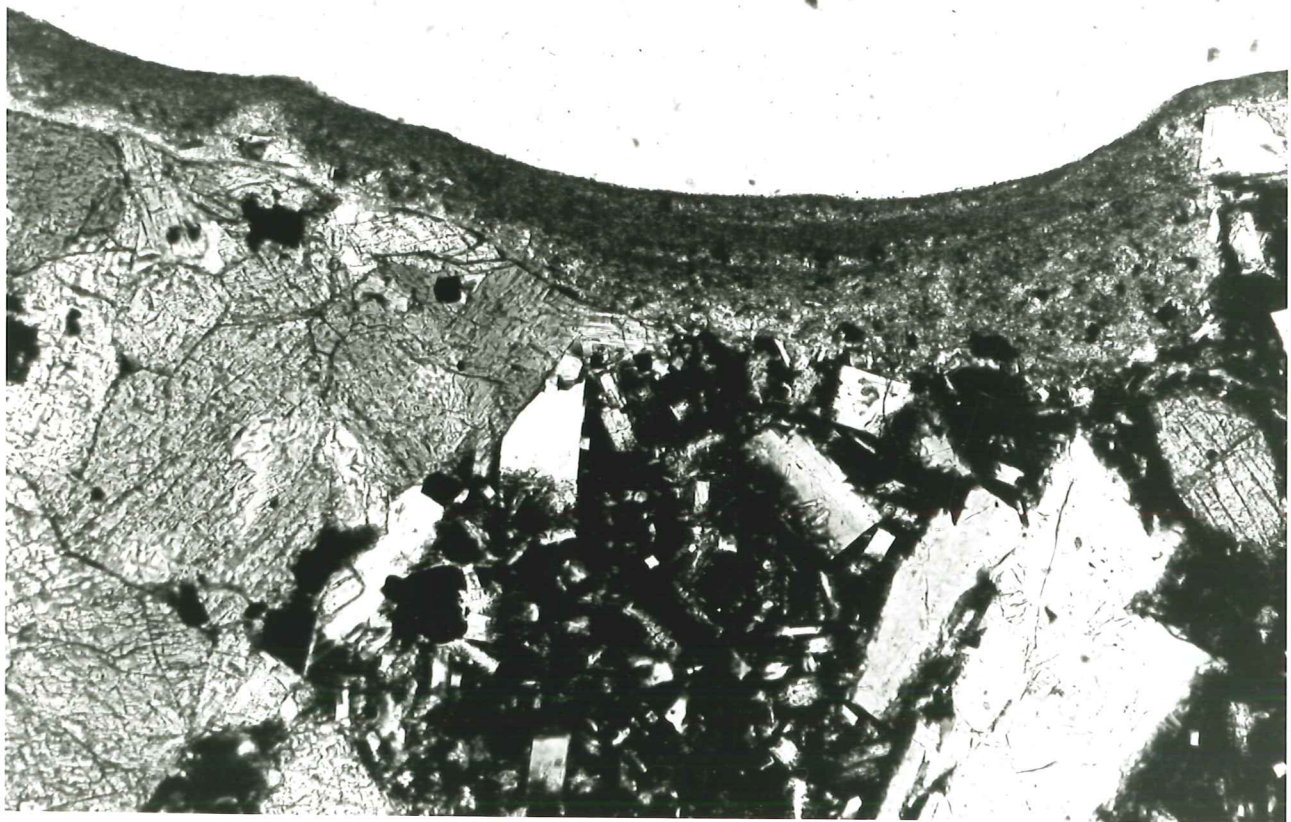
Some of the coatings of the Poás and the Rincón de la Vieja are partially effected by chemical erosion. The upper layer has partly disappeared and remnants of it are present as caps at the coating surface.

3.2.2 *Micromorphology on thin sections of coatings*

Micromorphological observation reveals that coatings found on the four different volcanoes are fairly similar in morphology. The coatings are convolute, dominantly compound layered and laminated. The microlayers consist of a mixture of translucent, colourless to very pale yellow, isotropic, fine textured material and anisotropic mineral, silty, primary grains in different amounts. The isotropic appearance and the translucent internal fabric of the fine textured groundmass indicate that this material is amorphous and secondary formed. We speculate that the secondary formed isotropic material resulted from weathering of fine ash particles.

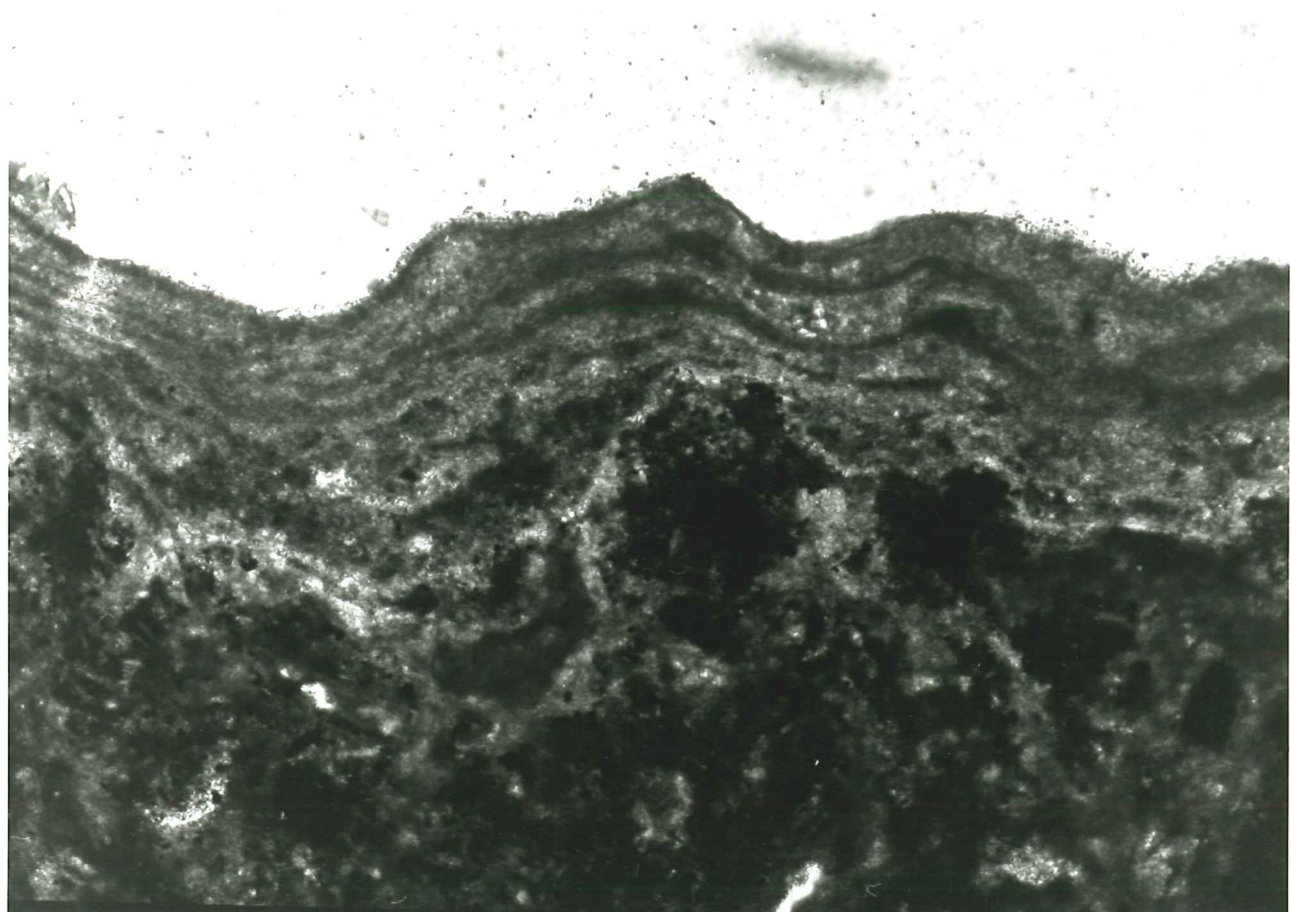
The boundary between the different microlayers is generally gradually. The thickness of the layers varies, even within one layer. Coatings are thinner, with a dominant composition of isotropic material at extending parts of the parent material, and thicker in micro depressions (see picture 1, p11). In these depressions very fine primary mineral fragments are accumulated as a result of microtransport of the volcanic ash at the rock or ash surfaces. Different layers dominantly composed of primary minerals may alternate with layers consisting of isotropic material (pictures 1, 2, 3a and 3b, resp p11 and p12). This is an indication that formation of the isotropic material and accumulation of fine ash are nearly simultaneous processes, which are basically responsible for the coating formation.

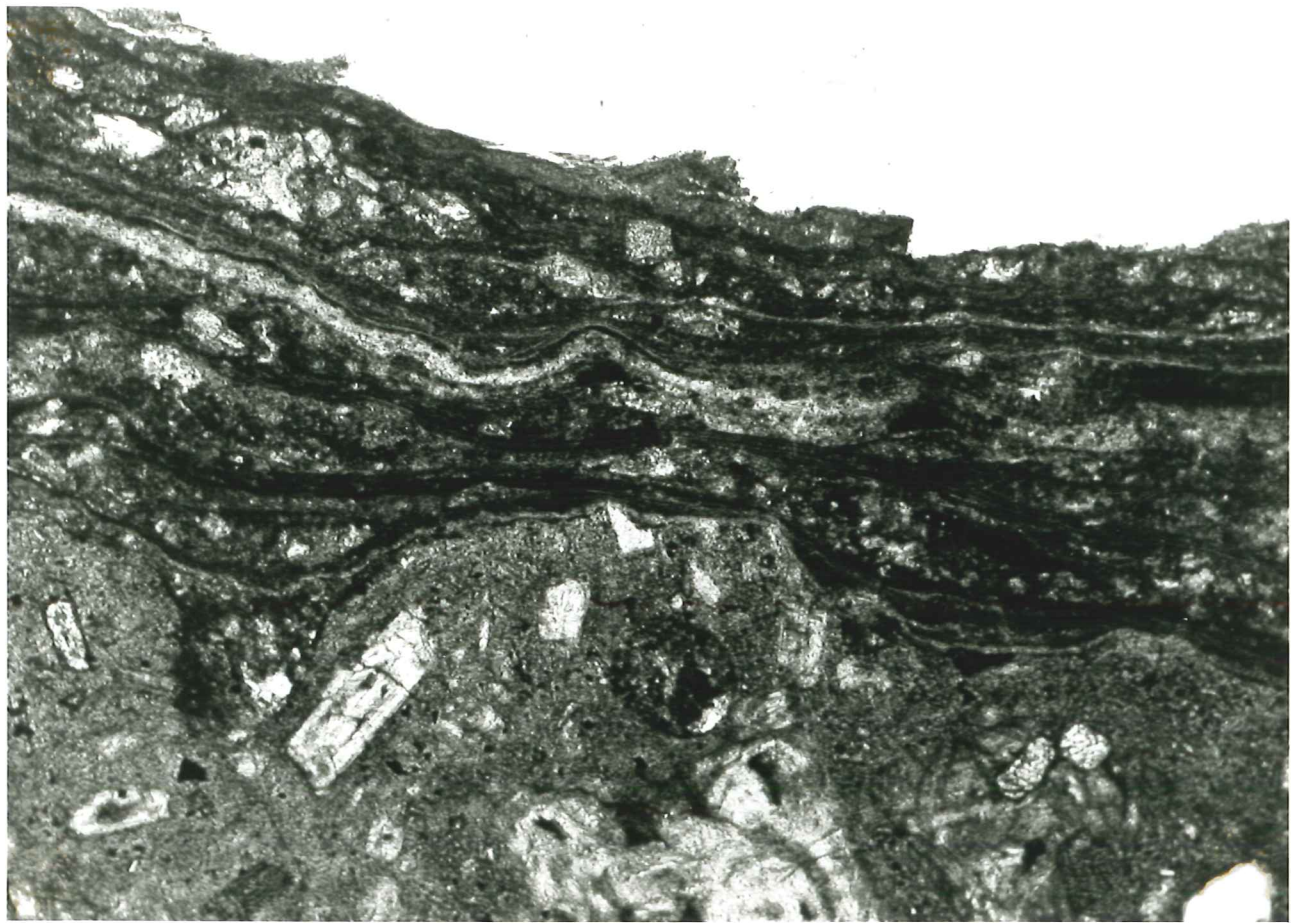
The total thickness of the coatings ranges from about 100 µm up to 8 mm. The



Picture 1. Coating at surface of rock fragment (Arenal). The coating is thicker in the microdepression, where alternate layers are visible of more granular and more isotropic material. (magn 270x)

Picture 2. Coating at surface of ash/scoria (Poás). Alternate layers are visible. (magn 270x)





Picture 3a and 3b. Coating at rock fragment (Rincón de la Vieja). The alternate layers are accentuated by red iron colour. Mineral grains are incorporated in the layers. Picture 3b shows signs of chemical erosion: the upper layer is partly dissolved and in the coating are solution hollows visible. (magn 94 x)



average thickness is between 1 and 2 mm. However, the pendants can be up to 15 mm thick.

The coatings originating from the four different volcanoes do not differ largely in appearance, although there are some minor distinctions. The coatings of the Arenal contain appreciable amounts of anisotropic very fine primary mineral particles. The coatings of the Turrialba contain more coarse primary mineral particles, and the micro layers are less distinct. The isotropic groundmass shows at some places a slight white-blueish colour with incident light (XPL), suggesting that the coatings consist of cryptocrystalline secondary silica (Brinkman et al., 1973).

The coatings of the Poás contain more iron and show the same opaline colour with crossed polarisers. The appearance of the coatings is generally less dusty as less of the fine mineral particles are incorporated.

The coatings of the Rincón are very thick, up to 8 mm and concluding from the reddish colour they contain iron. The microlayers are prominent, as they are accentuated by the reddish colour of the iron (pictures 3a and 3b, p12).

Micromorphological observations show chemical erosion at the coatings (picture 3b). Some of the outer margins of the rock fragments directly underlying the coating display weathering features. Phenocrysts of plagioclase are completely altered. In the weathering voids fine textured, translucent, isotropic material occurs.

3.2.3 Submicroscopy

-SEM-EDXRA on coatings in uncovered thin sections

Microchemical analysis of the SEM-EDXRA in uncovered thin sections demonstrate that Si and O are the dominant elements present in the fine textured, isotropic, translucent groundmass of the coatings accompanied by small amounts of Al. Occasionally traces of Fe and Ti were detected. The micro-chemical data for Si and Al were converted to semi-quantitative mass percentages. The averaged data found for the groundmass of the coatings are given in table 3.

Table 3. The averaged EDXRA data of Si and Al in found in the coatings of the four volcanoes (mass%).

	Arenal	Turr.	Poás	Rincón
N	22	28	17	27
-----mass%-----				
Si	33.7	35.8	38.8	38.1
sd ^{..}	2.0	4.1	3.1	3.9
Al	3.5	2.8	1.8	2.7
sd	1.4	1.6	0.8	0.9

* N = number of observations

** sd = standard deviation

From this table we can conclude that the data do not differ significantly for the different volcanoes.

The fine (2-50 μm) mineral particles present in the coatings of the Arenal consist of primary minerals, as microchemical analysis at these grains reveal the presence of Al, Si, Ca, Na and Fe.

From these chemical data and the micromorphological observations can be concluded that the groundmass of the coatings consist dominantly of amorphous silica. This silica is probably liberated by weathering of primary material, especially coloured volcanic glass in the fine fraction of volcanic ash present at the surface of the soil and rock fragments.

-SEM-EDXRA carried out on rough coating surfaces

SEM and EDXRA were also performed at rough surfaces of coatings of the four volcanoes and at a vertical cross section of a coating of the Rincón de la Vieja. The coatings consist of very fine primary mineral grains and fine textured material. The majority of the grains are accumulated in micro depressions present at the rock and soil surfaces. Fine textured pure material covers the particle surfaces as a glaze and fills the intergranular spaces between the particles (picture 4, p15). Chemical spectra reveal that the fine textured material dominantly consists of Si. Figure 2 (p16) gives the chemical spectra for the spots indicated in pictures 4-6 (p15-17). Primary mineral grains consist of Si, Al, Na, Ca and Fe. The primary mineral grains are cemented by the siliceous fine material and together the materials form the hard, thin coatings at soil and rock surfaces.

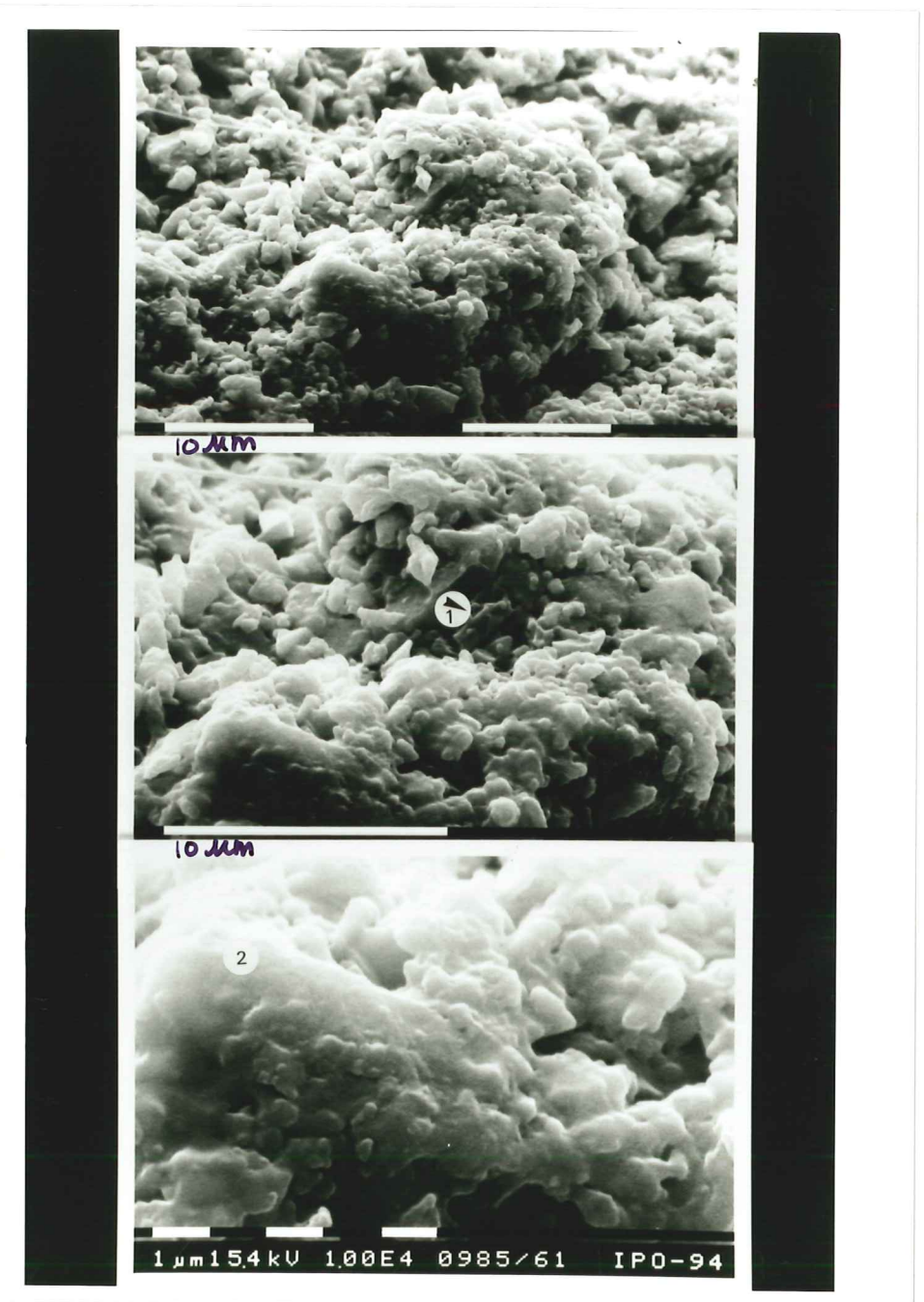
Chemical erosion of the upper layers of coating can take place, according to the SEM pictures (picture 5, p16). This is in agreement with the optical observations at the different levels.

The vertical section of a coating of the Rincón de la Vieja shows different layers with a gradual transition (picture 6, p17). The layers vary largely in density and texture. Some layers are very dense, while others consist of grains that are cemented together. The latter are highly porosive, probably as a result of chemical erosion. Repeated EDXRA at the cross section and surface of grains in these layers shows that all grains and the fine textured material consist of silica.

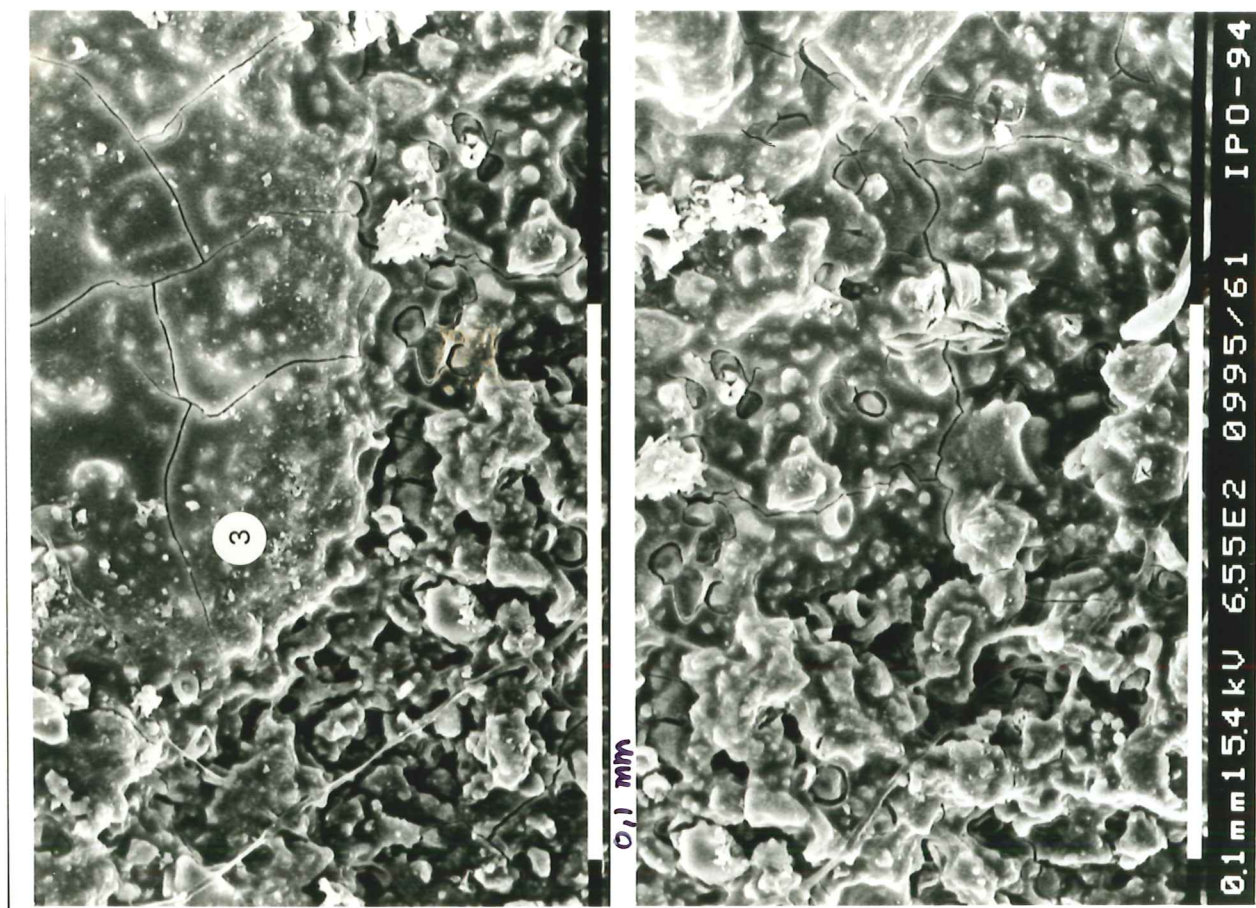
The observations suggest again that formation of the amorphous fine textured material occurs simultaneously with accumulation of fine mineral particles. The fine mineral particles partially or totally weather and contribute to the formation of the secondary silica, which cements the remaining mineral particles.

Upon continuous weathering all mineral grains in the coatings may weather isovolumetrically and silica pseudomorphs can be formed after primary mineral grains.

Convolute, laminated, compound coatings are found that consist dominantly of amorphous silica. Varying amounts of ash can be incorporated as the accumulation of volcanic ash and the formation of the amorphous material take place simultaneously. The amount of ash incorporated is dependent to the micro relief of the coating. These coatings are found in horizontal and vertical position both at the soil surface and at the surface of rock fragments. In situ weathering is not the only determining factor, as the coatings can occur at wood fragments. Chemical and physical erosion of the coatings can take place. the formation of the coatings will take place in order of years.



Picture 4. SEM picture of a coating at the Arenal in three magnifications. Grains are visible in the microdepressions. These grains are incorporated in and covered with the siliceous material. The numbers in the pictures correspond with the chemical spectra in figure 2.



Picture 5. Surface of a coating with low relief. The coating is subject to chemical erosion, as the upper layers partly have disappeared already.

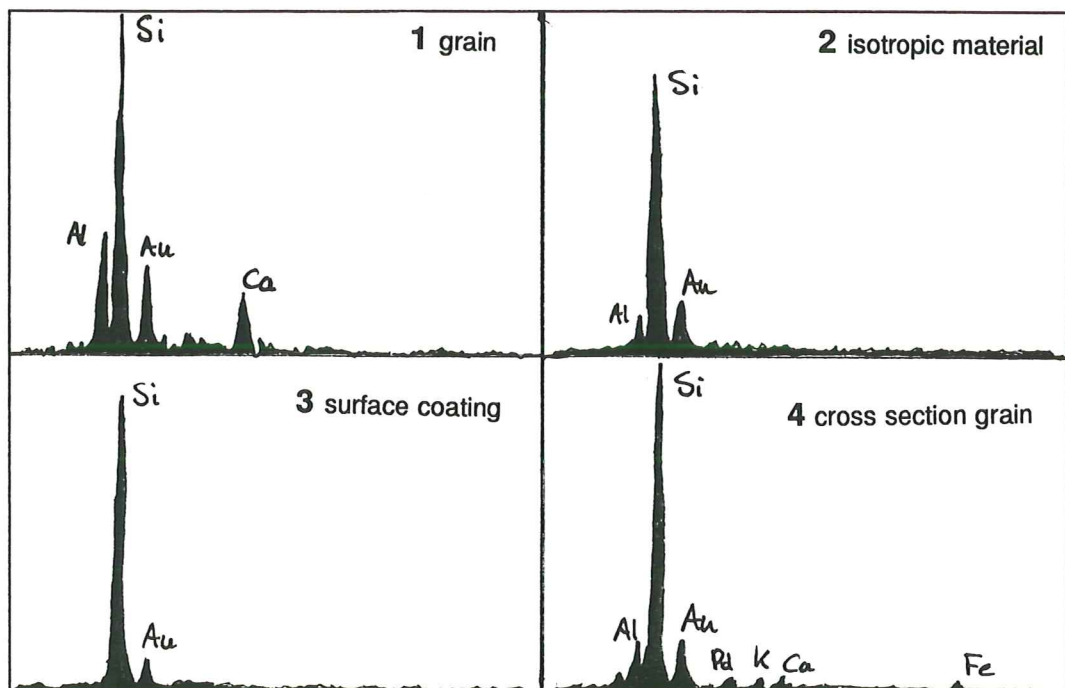
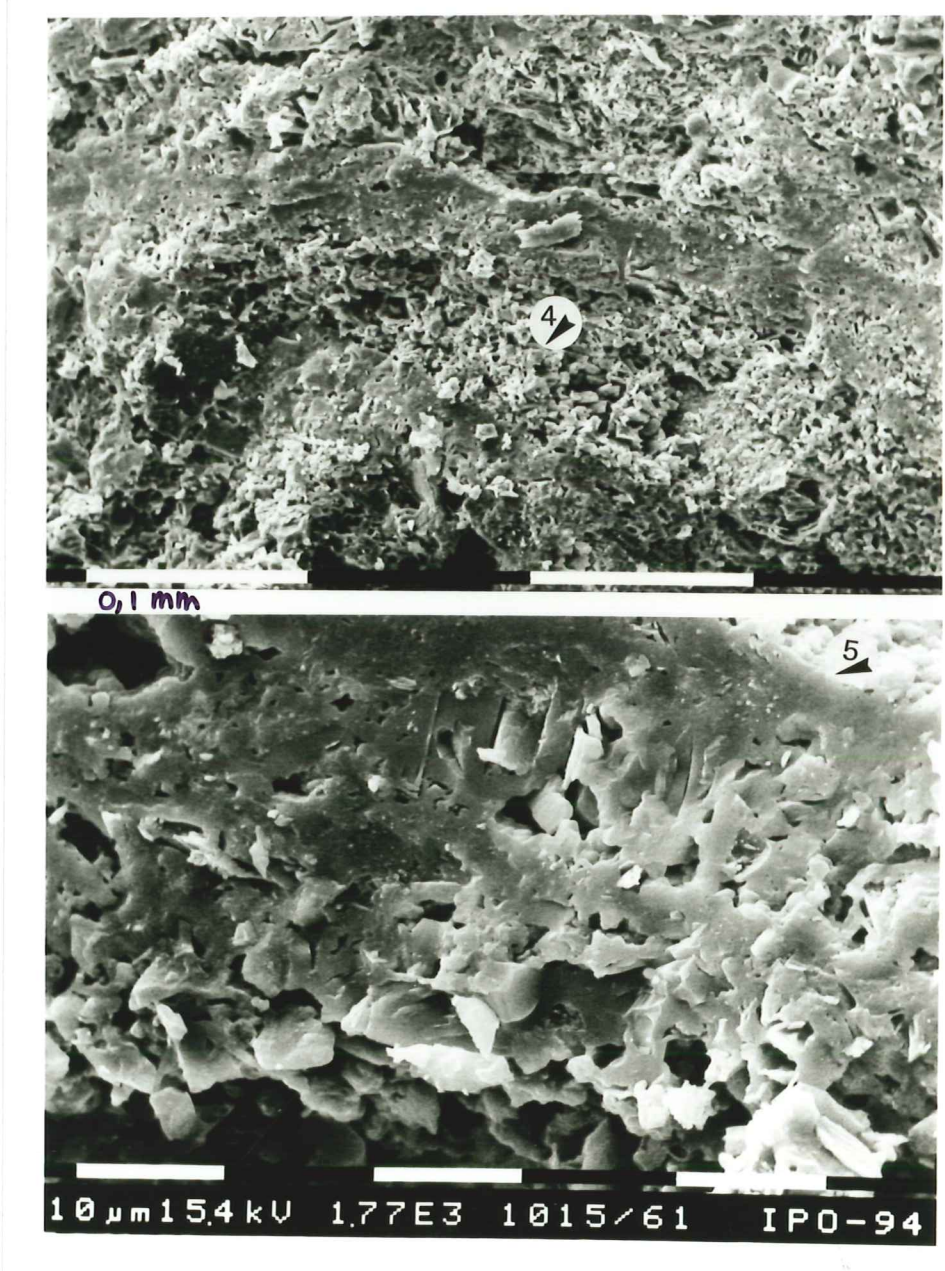


Figure 2. Chemical spectra (SEM-EDXRA) corresponding with the numbers on pictures 4-6.



Picture 6. Vertical cross section of a coating at the Rincón de la Vieja. Different layers with alternating density are seen. The grains in the highly porosive granular layers are completely silicified.

In the next chapter will be considered whether the chemical conditions found at the volcanoes favour a coating genesis as presented in this chapter. A weathering experiment will be done to follow the weathering process and study the effect of the acid conditions.

4 CHEMICAL RESULTS AND INTERPRETATION

4.1 Chemistry of solid material

4.1.1 XRF analysis

The results of the XRF- analysis are given in the table 4. From these data can be concluded that the chemical composition does not differ significantly within the different fractions.

Table 4. Elements present in the different fractions and bulk of volcanic ash of the Arenal. Elements are represented as mass fractions of oxide components.

fraction	SiO ₂ %	TiO ₂ %	Al ₂ O ₃ %	Fe ₂ O ₃ %	MnO %	MgO %	CaO %	Na ₂ O %	K ₂ O %	P ₂ O ₅ %	BaO %
I	52.66	0.86	19.29	7.73	0.14	4.27	8.84	3.70	0.60	0.13	0.05
II	53.93	0.87	19.35	7.96	0.15	4.98	8.79	3.50	0.59	0.13	0.04
III	54.67	0.89	18.05	8.50	0.16	5.89	8.28	3.43	0.59	0.14	0.05
IV	54.68	0.90	17.42	8.81	0.17	6.27	7.86	3.45	0.62	0.15	0.05
V	54.62	0.87	18.80	7.90	0.15	4.84	8.33	3.68	0.65	0.16	0.05
bulk	54.33	0.91	17.92	8.61	0.16	5.94	8.25	3.48	0.61	0.15	0.05

Volcanic glass, especially coloured glass contains appreciable amounts of Na, K, Al, Fe, Ca and Mg (Shoji et al., 1993). The concentrations of these cations in the glass can vary largely. As a result it is not possible to draw conclusions from this data with respect to the amount and mineralogy of minerals in the ash.

4.1.2 Guinier diffraction pattern

Coating material present on a rock surface was sampled with a dentist drill. With a Guinier camera a diffraction pattern was made of this material. The pattern showed the presence of plagioclase from the incorporated ash particles. Comparison with diffraction patterns of standard minerals showed that the plagioclase in the volcanic ash is a variety very near to anorthite, which means that it contains dominantly Ca and little or no Na. Ca-plagioclase appears to be the main component in the volcanic ash.

No other crystalline material could be detected, which suggests that the fine textured material of the groundmass of the coating is amorphous. This conclusion is in agreement with the micromorphological observations.

4.2 Chemistry of solutions

4.2.1 Field water sample analysis

The origin of the water samples taken in the field samples is given in table 5 (annex 1). The analysis of the samples is given in table 6a and 6b (annex 2). A few things can be deduced from these tables. The pH of the samples ranges from 2.51 to 4.99, with the pH of 6.38 (sample AW9) as an exception. The low pH found in the other of the samples is probably caused by condensation of the gases emitted by the volcano as referred to before (chapter 2.1.7). Concluding from the high Cl⁻ and SO₄²⁻

concentrations, HCl and SO₂ are the most important acidifiers at the volcanoes studied. The sample with pH of 6.38 is taken at two km's from the crater (AW9), of which can be concluded that the influence of the gases decreases rapidly as the distance from the crater increases.

Apart from this high H⁺ concentration which is found in the majority of the samples, SiO₂, Al, Na, Mg and Ca are the dominant cations which are present in high concentrations. Weathering in this environment takes place under extremely acid conditions, which may result in a high weathering intensity. The high concentrations found are in agreement with this idea.

The SiO₂ is thought to originate mainly from volcanic glass and plagioclase, as these minerals are present in large amounts and the most easily weatherable minerals as we have seen in chapter 2. A very small amount may originate from other minerals. The cations found in the solution may all originate from the volcanic glass and in minor amounts from other primary minerals.

To examine whether there are clearly distinct types of solutions found at the four volcanoes with respect to the ratios between SiO₂, Na+K and Ca+Mg, the concentrations of these cations found in the samples are plotted in a triangle graph (see figure 4).

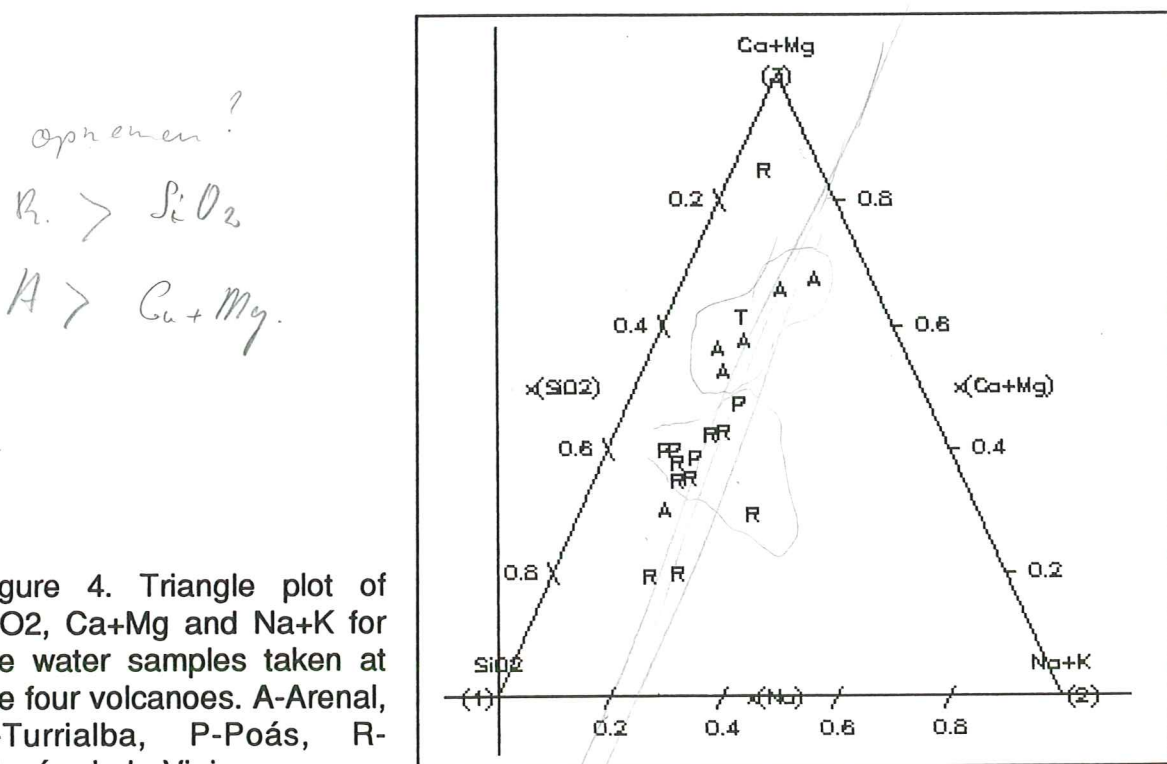


Figure 4. Triangle plot of SiO₂, Ca+Mg and Na+K for the water samples taken at the four volcanoes. A-Arenal, T-Turrialba, P-Poás, R-Rincón de la Vieja

In this figure we can see that all samples taken in the field are characterized by low Na+K values relative to SiO₂ and Ca+Mg. There seems to be a trend in these data, as they are all on a imaginable line. However, the patterns for the four volcanoes are not very distinct. If we have a look at the clusters of samples of the different volcanoes, the cluster of the Arenal samples and the one sample of the Turrialba are

shifted to more Ca+Mg, the centre of the Rincón cluster tends to more SiO₂, while the Poás cluster is situated in between. As is described before, the ash deposits most recent are found at the Arenal and Rincón de la Vieja. There is no apparent relation in the triangle graph between the age of the volcanic ash and the position of the samples from the four volcanoes in the diagram. From this can be concluded that the trend that seems to be found is at least not related to the age of the weatherable material for the different volcanoes as a whole.

Sample AW2 is a precipitation sample that is directly filtered. Sample AW3 is taken exactly from the same solution, but is not filtered immediately. The solution has been able to weather the fine volcanic ash included for about one month. Result of this weathering is a decrease in H⁺ concentration, and an increase in SiO₂, Al and Ca. *pH pH 3*

Samples AW11 and AW12 are taken in moss and from under a coating, and it can be assumed that these samples have had more time to come into contact with volcanic ash and that the water may be already partially evaporated. Especially in AW11, the Si, Na, Ca and Al are high relative to the other samples of the Arenal. These are partially the same cations as were found before to be liberated with the weathering in the not filtered sample. We assume for the moment that Si, Al and Ca and to a minor extent Na and Mg are the main cations liberated with weathering of the volcanic ash of the Arenal.

4.2.2 Analysis solutions weathering experiment

The analysis of the solutions obtained from the weathering experiment with acid solutions are given in table 7 (annex 3). The concentrations of H⁺, SiO₂, Al and Ca and Na found with the repetitions are graphically presented in figure 5a-e (annex 4). Except for the hydrogen concentration which shows the opposite, highest concentrations of cations are found in the solutions from fraction I (which is the finest fraction), and lowest in solutions from fraction V. This is due to the specific surface which increases with decreasing grain size. The concentrations of the solution of the bulk sample give a good weighed average of the different fractions.

With weathering, H⁺ ions are used in reactions involved with the dissolution of material (alkalizing effect; Bolt and Bruggenwert, 1976). The primary reactions in the dissolution of volcanic glass involve the consumption of H⁺ ions. Therefore the weathering rates are dependent on the hydrogen ion concentration. (Shoji et al., 1993) This means that the amount of consumption of H⁺ ions is a measure for the weathering that has taken place.

The H⁺ concentration of the acid solution was originally 1 mmol/l (pH 3). This concentration has decreased most after the first shaking session. With the following repetitions it decreases less. Concluding from this, weathering is most intense in the first session and decreases subsequently. The trends for the other solutes, although not always very distinct, are increasing for Si and Al and decreasing or staying rather at the same level for Ca and Na. This could be explained by the fact that coloured glass, which is assumed to be the most weatherable material in the volcanic ash, contains a large concentration of cations that lead to substitution of Si. This substitution weakens the bonding characteristics of the glass because there are fewer silica-silica linkages. Cations are susceptible to rapid removal from the both the surface from the glass and within the glass by ion exchange with H⁺ ions. Removal of cations weakens the glass and increases the porosity of the glass which makes it

more susceptible to dissolution. (Shoji et al., 1993)

If this process is occurring, it should become visible if the data are plotted in a triangle plot of SiO₂, Na and Ca+Mg.

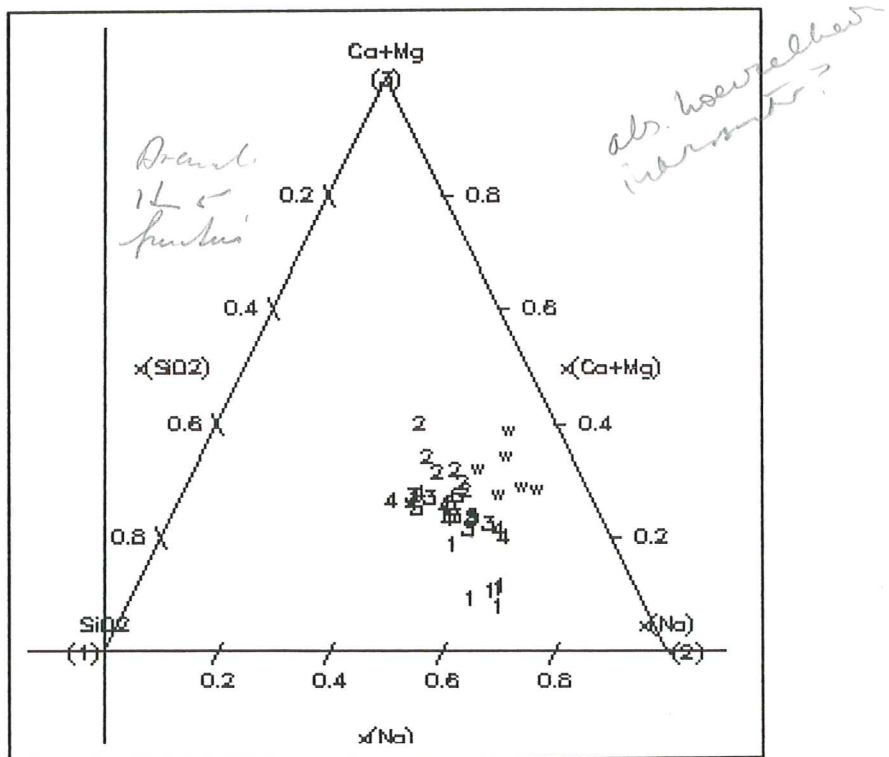


Figure 6. Triangle plot of SiO₂, Ca+Mg and Na ratios in solutions obtained with weathering experiments. 1-5: solutions of the successive repetitions of the shaking sessions, w: solutions from the experiment with water.

Figure 6 represents this graph for the solutions of the weathering experiment with acid. The K data are left out of consideration, as they vary too much. The data are characterized by relative low Ca+Mg, and high Na content; while SiO₂ is present in varying amounts. The solutions are numbered according to the repetition of the shaking sessions. The trend we would like to observe would be a shift towards more silica and less of the cations. What we see in this figure is that silica is relatively stable, Na decreases and Ca+Mg increases. From this we can conclude that the process of partial dissolution is not very clear in this experiment, although there are indications leading in that direction.

However, another process may be taking place, regarding the trend towards decreasing Na and increasing Ca. There may be a preference order in the weathering of the cations from the glass. Na seems to be dissolved rapidly, whereas Ca takes a longer time and becomes more important with repeated shaking sessions. White and Claassen (1980) report a succession of weathering of coloured volcanic glass with Na dissolving before K.

In table 8 (annex 5) is given the analysis of the solutions which were shaken with distilled water for 7 days. Al is not present; if liberated by weathering, it precipitates immediately at this pH. The concentrations of SiO₂, K, Mg are much lower than in the experiment with acid. This is considered to be an effect of a lower weathering rate due to higher pH. However, Na and Ca reach high values. Although anorthite, the Ca-variety of plagioclase, is able to weather under the circumstances

found in the water experiment (see calculation in appendix 1), the high concentration of Na cannot originate from this feldspar, as it contains little or no Na. Therefore we assume that the majority of both Na and Ca originate from coloured volcanic glass. If this is true, it could mean that the Na and Ca are the first components of the glass to weather under these conditions. The solutions are represented in the triangle graph of figure 4.

If we compare the acid solutions in this figure with the solutions obtained with the weathering experiment, less silica is found and the ratio between Na and Ca+Mg is shifted somewhat to the Ca+Mg side. This solution has been shaken with the ash for 7 days, probably long enough for Ca to dissolve from the volcanic glass next to Na.

What we have seen so far in the experiment is that weathering of the ash occurs while shaking it. This weathering is more intense under acid conditions and the finest textured fraction weathers most easily. With weathering of probably dominantly volcanic glass, H^+ ions are consumed and Al, SiO_2 , Ca, Na (and Mg) ions are liberated. There seems to be a preferential order in which the cations dissolve, with Na as the first ion.

If we compare the data of table 6 and table 7 (resp. annex 3 and 4), we have to focus on the ratios between the different cations, as the absolute concentrations are dependent on the contact time, which is unknown for the samples taken in the field. Therefore we compare the triangle plots of the water samples from the field, and the solutions obtained with the experiments.

Figure 4 and figure 6 show large differences. The material used for the weathering experiment consists of volcanic ash of the Arenal, so we have to concentrate on the samples of the Arenal in figure 4. The difference is mainly a shift towards more Na in the weathering experiment. As we have seen before the Na has to originate from the glass. We found indications that Na is the first cation to dissolve from the glass. The difference in Na content between field and experiment could then be explained by the fact that the material which weathers in the field is already partly weathered and has lost part of the Na already. In addition, in the field weathering of feldspar will contribute to a larger extent to the composition of the solution, which enlarges SiO_2 , Al and Ca concentrations, and consequently reduces the Na portion.

4.3 Neoformation

After studying the weathering process, some calculation will be done towards the possibilities of formation of new material. Minerals that may form from the solutions with high silica and aluminum concentrations found, are gibbsite and kaolinite. However, rapid weathering can release elements faster than crystalline material can form. As a result the solution can become oversaturated with respect to poorly ordered solid-phase materials, like allophane and imogolite. (Shoji et al., 1993)

In the following paragraphs the formation of the different minerals/materials will be discussed with regard to the conditions found in the field and experiment.

4.3.1 *Allophane and imogolite*

The formation of imogolite and allophane is not expected under these conditions, as these materials are usually not formed below pH values less than 5. At

Waarom moet de pH \downarrow bij lage pH
geen overgangszone

these low pH values Al can be complexed in humus complexes. (Shoji et al., 1993, Mizota and van Reeuwijk, 1989) However, at the bare surface at the summit of the volcanoes studied, hardly any vegetation is found. Still, we have not observed allophane or imogolite. We do not have an explanation for this.

4.3.2 Gibbsite

Al can form complexes in water, which are pH dependent (Bolt and Bruggenwert, 1976). With the aid of stability constants the equilibria are calculated for this situation (see annex 6). From these calculations we can conclude that Al will be predominantly present in dissociated form and the Al concentration is only slightly influenced by complexation. In the annex the activity of Al was calculated and plotted against the pH in a solubility diagram. From this we can conclude that gibbsite is not formed under the conditions found in the experiment.

4.3.3 Kaolinite

Values for the equilibrium constant for the formation of kaolinite from the literature vary largely. The values for $\log K$ range from 2.0 (Garrels and Christ, 1965) to 7.63 (Bolt en Bruggenwert, 1976).

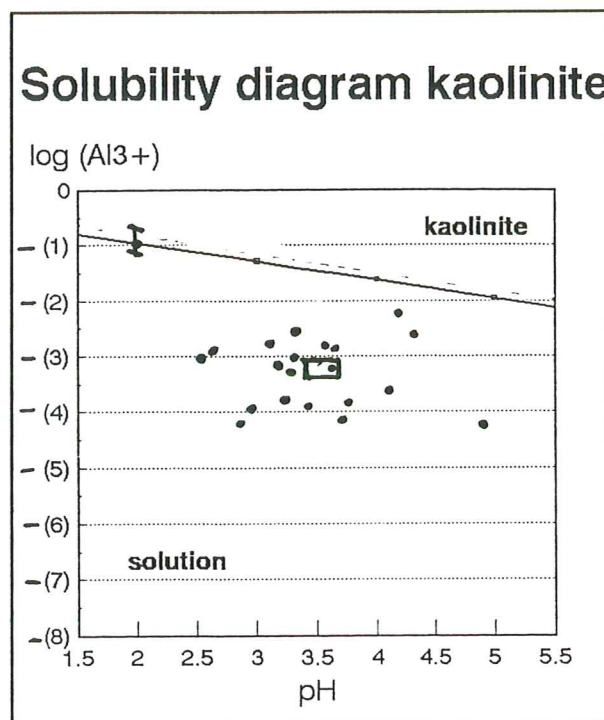


Figure 7. Solubility diagram of kaolinite, constructed for $\log H_4SiO_4$ value of 3.70. The deviation of the line for $\log H_4SiO_4$ values found in the samples in the field is indicated. Samples from the field are indicated with a dot, the range of the solutions of the weathering experiment (with acid) with an asterisk.

Figure 7 represents a solubility diagram for kaolinite, constructed for a fixed concentration for SiO₂ in solution ($\log H_4SiO_4 = 3.70$), using $\log K = 5.71$ (Robie et al., 1978). If we plot the concentrations of the water samples from the field and of the solutions of the weathering experiment in this diagram, it appears that the chemical conditions for the formation of kaolinite are not present. However, although with the $\log K$ of 2 the solutions are positioned above the solubility line, the formation of kaolinite takes time and is usually not found in very young soils.

4.3.4 Amorphous silica and aluminum

The equilibrium constant of amorphous silica is lower than that of quartz (resp. -4.00 and -2.74; Bolt and Bruggenwert, 1976). Harder and Flehmig (1969) conclude that precipitation of quartz can take place only from those solutions which are undersaturated with respect to amorphous silica.

From equation (1) can be calculated that amorphous silica can precipitate as the SiO_2 in solution (silicic acid: H_4SiO_4) reaches a concentration of about 1.82 mmol/l. The samples taken in the field do not reach this concentration, but samples AW11, AW12 and PW3 come rather close.



$$(\text{H}_4\text{SiO}_4) = 10^{-2.74} \Rightarrow 1.82 \text{ mmol/l}$$

Quartz can already precipitate at a H_4SiO_4 concentration of 0.100 mmol/l. This means that the solutions found at the volcanoes are oversaturated with respect to quartz (except for PW4 and RW9), and undersaturated with respect to amorphous silica. However, quartz is not found in the coatings. This may be a result of the other solutes (Al, Fe, Mg, NaCl, Na₂SO₄; Smale, 1973) that can have influence on the silica deposition. The precise mechanisms in solutions with compound composition are not known. A second and probably more plausible explanation is that the concentrations of solutes may be increased largely by rapid evaporation of the water caused by the high input of solar radiation. Considering the Costarican climate this is very likely. *OK.*

The saturation concentration of amorphous aluminum can be calculated in the same way as for amorphous silica. With $\log K = -32.34$ the equilibrium concentration is much higher (306.9 mmol+/l). This concentration is not reached by far in the field water samples, which may explain the few aluminum found in the coatings. Other minerals can be formed from the concentrated solutions, such as gypsum, which we indeed found as crystals at the Arenal.

Shoji and Masui (1971) report opaline silica as a product of the early stages of weathering of volcanic ash. It can be formed by precipitation from soil solutions that are oversaturated with silica due to surface evaporation. They refer to pedogenic silica, which is mentioned to occur only in the 0.2 - 5 μm size fraction. (Shoji et al. 1993)

4.4 Interpretation

Condensation of gases emitted by volcanoes can form acid precipitation in the direct environment, which results in acid soil (and surface) solutions. Rapid weathering can take place when these solutions come into contact with easily weatherable material. This process probably already starts in the air as very fine volcanic ash can be caught in by rain drops and precipitate with it. *OK*

Of the volcanic ash, the finest textured fraction weathers most easily. Coloured glass is most susceptible to weathering, where next to SiO_2 the (cat)ions liberated are

mainly Al, Ca and Na. Of these, Na seems to be liberated mainly in the early stage of weathering.

The weathering of the ash causes high concentrations of solutes in the soil solutions, especially of silica and aluminum. Na is less dominant in the solutions in the field, probably because the parent material is partly weathered already. If the concentrations are increased by evaporation of water from the solution, amorphous silica can precipitate at the surface. This amorphous silica forms the groundmass of the coatings we observed at the four volcanoes studied. Kaolinite, gibbsite, allophane and imogolite are not formed.

With rewetting of the precipitated material, probably part of it will dissolve again, especially as the solution is largely undersaturated with respect to the precipitates. This can form an explanation for the erosion we observed at the upper layers of some of the coatings. However, as there are coatings present, at this time the net effect at the places where they occur has been accumulation.

4.5 Coating genesis

The following process of coating formation is generated from the optical and chemical observations.

Active volcanoes produce gases which can form acid soil solutions and surface water upon condensation. The major acidifiers at the volcanoes in Costa Rica are SO₂ and HCl.

With eruptive activity of the volcanoes large quantities of volcanic ash are emitted. The ash contains large amounts of volcanic glass, of which especially the coloured glass is very susceptible to weathering.

The combination of the acid soil solutions and fine textured ash can result in rapid weathering, which produces high concentrations of solutes, especially of SiO₂ and Al in solution. If, at the surface, water evaporates from this solution, amorphous silica and some Al can precipitate. Allophane and imogolite are not formed under these acid conditions, while kaolinite is not formed due to the high dynamics of the environment.

During the process described above, continuous supply of volcanic ash takes place, which is accumulated in the (micro)depressions. There the ash can be incorporated in the amorphous material as it precipitates. This mixture of amorphous material and mineral particles forms the coatings present at the volcanoes.

Phases of formation can be alternated with phases of chemical erosion, which can accentuate the laminated character of the coatings. In addition, physical erosion can take place, especially at dynamic places at the soil surface. This whole process of formation and erosion can take place in a time span of years to decennia, which is extremely rapid for soil forming processes.

REFERENCES

Abbey, S., 1980. Studies in 'standard samples' for use in the general analysis of silicate rocks and minerals. Part 6: 1979 edition of usable values. Geol. Surv. Can Pap., 80-14: 30 p

Alfaro, Ma. del R., E. Fernández, J. Barquero, J.J. Rodríguez and M. Rodríguez, 1986, Lluvia acida de origen volcánico, Boletín de la vulcanología, 17, p.15-22

Alfaro, Ma. del R., J.J.Rodríguez, E. Fernández and J. Barquero, 1988. Acid deposition from natural sources, Arenal and Poas volcanoes. Revista Geofísica 29

Alvarado-Induni, G., 1993. Costa Rica, land of volcanoes. Costa Rica. Original title: Los volcanes de Costa Rica, Gallo Pinto Press, Costa Rica

Aomine, S. and K. Wada, 1962. Differential weathering of volcanic ash and pumice, resulting in formation of hydrated halloysite. Am. Miner., 47: 1042-1048

Bisdom, E.D., D. Tessier and J.F.T. Schouten, 1990. Micromorphological techniques in research and teaching, In: L.A. Douglas (ed), Soil Micromorphology: a basic and applied science. Developments in Soil Science 19: 581-603, Elsevier, Amsterdam, New York

Bolt, G.H. and M.G.M. Bruggenwert (ed), 1976. Soil Chemistry, Part A: Basic elements. Developments in Soil Science 5A, Elsevier, Amsterdam, Oxford, New York

Brinkman, R., A.G. Jongmans, R. Miedema and P. Maaskant, 1973. Clay decomposition in seasonally wet, acid soils: micromorphological and mineralogical evidence of individual argillans. Geoderma, 10: 259-270

Bullock, P., N. Fedoroff, A. Jongerius, G. Stoops and T. Tursina, 1985. Handbook for soil thin section description. Waine Research Publications, England, 150 p

Cheminee, J.L., H. Delorme, J. Barquero, G. Avila, E. Malavassi and F. Guendell, 1981. Some physical and chemical aspects of the activity of the volcanoes Poas and Arenal, Boletín de vulcanología, vol. 11: 12-16

Delvigne, J., 1965. Pédogenèse en zone tropical; la formation des minéraux secondaires en milieu ferrallitique. Mém. Orstom Ed. Dunod, Paris 13, 177 p

Fitzpatrick , E.A., 1970. A technique for the preparation of large thin sections of soils and consolidated material, In: D.A. Osmond and P. Bullock (ed), Micromorphological techniques and application. Techn. Monogr. 2. Soil survey of England and Wales, Rothamsted Exp. Sta., Harpenden, p 3-13

Garrels, R.M., and L.C. Christ, 1965. Solutions, minerals and equilibria. Harper and Row, New York, 450 p

Harder, H. and W. Flehmig, 1970. Quarzsynthese bei tiefen Temperaturen. Geoch. et cosmoch. acta, 34, 3: 295-305

Hartman, M., 1992. Estudio del posible riesgo de deslizamientos y procesos aliados en la cuenta del río Toro Amarillo, Turrialba, Costa Rica

Herrera, W., 1985. Clima de Costa Rica: Vegetación y clima de Costa Rica, volumen 2, San José, Costa Rica

Jongmans, A.G.M., 1994. Aspects of mineral transformation during weathering of volcanic materials: the microscopic and submicroscopic level, Wageningen, 143 p

Loughnan, F.C., 1969. Chemical weathering of the silicate minerals. Elsevier, New York, p 27-66

Malavassi, E., R. Alfaro, E. Fernández, J. Segura and J. Vindas, 1984. Lluvia ácida de origen volcánico en Costa Rica y su impacto. Primer congreso de geografía de Costa Rica, S.J., Costa Rica, 25 p

Miedema, R., T. Pape and G.J. van der Waal, 1974. A method to impregnate wet soil samples, producing high-quality thin sections. Neth. J. Agric. Sci. 22: 37-39

Mitchell, W.A., 1975. Heavy minerals. In: J.E. Gieseking (ed), Soil components, vol. 2. Inorganic components. Springer-Verlag, Berlin, Heidelberg, New York, p 449-480

Mizota, C., and L.P. van Reeuwijk, 1989. Clay mineralogy and chemistry of soils formed in volcanic material in diverse climatic regions. Soil Monograph 2, Isric, Wageningen, The Netherlands, 186 p

Nahon, D.B., 1991. Introduction to the petrology of soils and chemical weathering. John Wiley and Sons, New York

Nieuwenhuyse, A., A.G. Jongmans and N. van Breemen, 1994. Mineralogy of a Holocene chronosequence on andesitic beach sediments in Costa Rica. Soil Sci. Am. J. 53: 971-977

Robie, R.A., B.S. Hemingway and J.R. Fischer, 1978. Thermodynamic properties of minerals and related substances at 298.15 K and 1 bar (10^5 Pascals) pressure and at higher temperatures. U.S. Geol. Surv. Bull. 1452, 456 p

Shoji, S., M. Nanzyo and R. Dahlgren, 1993. Volcanic ash soils, genesis, properties and utilization. Developments in soil science 21. Elsevier, Amsterdam, London, New York, Tokyo

Allophane

Shoji, S., and J. Masui, 1971. Opaline silica of recent volcanic ash soils in Japan. *J. Soil. Sci.*, 22: 101-112

Shoji, S., I. Yamada and J. Masui, 1974. Soils formed from the andesitic and basaltic ashes. I. The nature of the parent ashes and soil formation. *Tokoku J. Agr. Res.*, 25: 104-112

Smale, D., 1973. Silcretes and associated silica diagenesis in Southern Africa and Australia. *J. Sed. Petr.*, 43, 4: 1077-1089

Soil Survey Staff, 1992. Keys to soil taxonomy. Soil manage. Support Serv. Tech. Monogr. 19, Pocahontes press, Blacksburg, VA

US Geology Survey, s.a., Open File Report 91-591, US Geological Survey, Vancouver

Velthorst, E., Manual for chemical water analysis, 1993, Department of soil science and geology, Agricultural University Wageningen.

Wada, K., Allophane and imogolite. In: J.B. Dixon and S.B. Weed (ed), Minerals in soil environments, 2nd ed., Soil Sci. Soc. of Am., Madison, WI, p 1051-1087

Weyl, 1980. Geology of Central America, 2nd ed., Berlin, Borntraeger, 371 p

White, A.F. and H.C. Claassen, 1980. Kinetic model for short-term dissolution of rhyolitic glass. *Chem. geol.*, 28: 91-109

Yamada, I., M.Saigusa and S. Shoji, 1978. Clay mineralogy of Hijori and Numazawa Ando soils, *Soil Sci. Plant Nutr.*, 24: 75-89

ANNEX 1

Table 5. The origin of the samples.

sample	volcano	site
AW2 1	Arenal	precipitation*
AW3 2	Arenal	precipitation#
AW5 3	Arenal	run-off stone
AW6 4	Arenal	soil
AW9 5	Arenal	precipitation 2 km's from volcano
AW11 6	Arenal	from under coating
AW12 7	Arenal	from out of moss
TW1 8	Turrialba	from puddle
PW1 9	Poás	puddle on a stone covered with coating
PW2 10	Poás	from puddle with ash
PW3 11	Poás	? river inside crater
PW4 12	Poás	run off from coating surface
RW1 13	Rincón	puddle
RW2 14	Rincón	puddle
RW3 15	Rincón	puddle in drainage gully
RW4 16	Rincón	puddle in drainage gully
RW5 17	Rincón	puddle on stone*
RW6 18	Rincón	soil solution under coating
RW7 19	Rincón	soil solution under coating
RW8 20	Rincón	precipitation collected with gutter*
RW9 21	Rincón	precipitation collected with gutter*

* This sample contained a small amount of fine ash, but was filtered with a rhizon sampler after a few days

This sample contained a small amount of fine ash and was not filtered

R = run off

P = precipitation

S = soil

R = run off from stones / coating

(drainage under coating, the coating layer)

R_P = run off water collected in puddles.

(coating layer solid phase - water from rainwater layer)

S = soil: water collected from uncoated solid material. (Layer under coating)

ANNEX 2A

Table 2a. Chemical analysis of the water samples taken in the field.

SAMPLE	pH	SiO ₂ mmol/l	H mmol+/l	K mmol+/l	Na mmol+/l	Ca mmol+/l	Mg mmol+/l	Al mmol+/l
AW2 p	2.83	0.353	1.479	0.066	0.736	2.070	0.317	1.880
AW3 p	3.32	0.722	0.479	0.062	0.690	2.500	0.334	3.150
AW5 r	3.58	< 0.200	0.263	0.007	< 0.065	0.328	0.018	0.672
AW6	4.99	0.589	0.010	0.021	< 0.138	0.280	0.040	0.068
AW9 *	6.38	0.000						
AW11 s	4.15	1.620	0.071	0.058	0.878	3.205	0.235	5.990
AW12	4.28	1.310	0.052	0.054	0.498	1.921	0.130	2.230
TW1	4.02	< 0.134	0.095	0.009	< 0.059	0.196	0.121	0.262
PW1	2.51	< 0.476	3.090	0.040	< 0.134	0.300	0.105	0.977
PW2	2.80	< 0.124	1.585	0.007	< 0.019	0.087	0.012	0.104
PW3	3.24	1.180	0.575	0.053	0.236	0.717	0.247	0.729
PW4	3.27	< 0.061	0.537	0.017	< 0.019	0.079	0.007	0.182
RW1 p	3.43	< 0.112	0.372	0.007	< 0.041	0.089	0.028	0.124
RW2	3.34	> 0.955	0.457	0.031	> 0.237	0.510	0.230	0.915
RW3	3.21	< 0.598	0.617	0.022	0.159	0.270	0.139	0.549
RW4	2.92	< 0.037	1.202	0.005	0.024	0.020	0.007	0.070
RW5	2.76	< 0.346	1.738	0.037	0.145	2.830	0.071	1.160
RW6	3.61	0.649	0.245	0.028	0.206	0.410	0.069	1.760
RW7	3.54	0.580	0.288	0.028	0.269	0.570	0.073	2.420
RW8	3.72	0.082	0.191	0.006	[0.017]	0.020	0.005	0.080
RW9	3.86	0.085	0.138	0.008	[0.025]	0.020	0.009	0.120

* Van dit monster was niet voldoende aanwezig om alle metingen te doen

of precipitate samples

= run-off from boulders and rocks' surfaces.

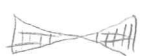
\$ = soil solution sampled directly underneath stones

= soil solution from sample from mesoph. low containing ^{abundant} very ^{abundant} particles.

ANNEX 2B

Table 6b. Continuation of chemical analysis of the samples taken in the field.

SAMPLE	Fe	Mn	NH4	Cl	NO3	SO4	H2PO4
	mmol+/l						
AW2 P	0.056	0.010	0.028	4.600	0.050	2.240	0.093
AW3 P	0.084	0.010	0.021	4.430	0.003	2.200	0.095
AW5 R	0.003	0.000	0.003	1.020	0.006	0.226	0.006
AW6 S	0.265	0.003	0.031	0.529	0.000	0.214	0.000
AW9*				0.653	0.017	0.286	0.000
AW11 S	0.009	0.007	0.002	6.740	0.000	2.460	0.000
AW12 S	0.001	0.004	0.000	3.090	0.000	1.840	0.000
TW1 P	0.001	0.001	0.005	0.036	0.000	0.683	0.000
PW1 R P	0.158	0.002	0.034	5.950	0.000	0.540	0.003
PW2 R P	0.007	0.001	0.012	1.940	0.000	0.147	0.000
PW3 R	0.008	0.002	0.001	0.826	0.000	1.680	0.000
PW4 R	0.002	0.000	0.023	0.647	0.014	0.205	0.001
RW1 R P	0.000	0.001	0.001	0.233	0.000	0.459	0.000
RW2 R P	0.005	0.004	0.002	0.763	0.000	1.622	0.000
RW3 R P	0.006	0.003	0.000	0.641	0.000	0.969	0.000
RW4 R P	0.011	0.000	0.000	1.000	0.000	0.304	0.000
RW5 R	0.195	0.001	0.042	1.150	0.000	5.190	0.000
RW6 S	0.003	0.000	0.005	1.030	0.000	1.580	0.000
RW7 S	0.002	0.000	0.011	1.370	0.000	1.960	0.000
RW8 R	0.003	0.000	0.002	0.098	0.000	0.232	0.000
RW9 R	0.002	0.000	0.012	0.199	0.000	0.164	0.000



waara
 hogere Cl
 is
 in de bodemwater
 dan in de grondwater?

ANNEX 3

Table 7. Chemical analysis of the solutions of the weathering experiment with acid solution.

SAMPLE	pH	SiO ₂	H	K	Na	Ca	Mg	in mmol+/l (SiO ₂ in mmol/l)	
								Al	Fe
z2 1	3.60	0.165	0.254	0.070	0.382	0.077	0.004	0.512	0.001
z3 1	3.55	0.146	0.281	0.008	0.349	0.059	0.004	0.473	0.001
z4 1	3.53	0.131	0.297	0.029	0.232	0.037	0.003	0.439	0.001
z5 1	3.51	0.131	0.308	0.032	0.318	0.058	0.004	0.459	0.002
zt 1	3.61	0.154	0.246	0.017	0.375	0.043	0.004	0.491	0.001
z1 2	3.77	0.230	0.172	0.003	0.340	0.360	0.018	0.613	0.002
z2 2	3.63	0.197	0.234	0.034	0.304	0.236	0.011	0.592	0.002
z3 2	3.55	0.170	0.283	0.017	0.365	0.222	0.009	0.549	0.006
z4 2	3.49	0.150	0.326	0.033	0.310	0.188	0.009	0.480	0.008
z5 2	3.48	0.152	0.328	0.016	0.310	0.211	0.011	0.480	0.009
zt 2	3.58	0.177	0.261	0.014	0.265	0.228	0.009	0.538	0.008
z1 3	3.73	0.220	0.186	0.002	0.287	0.188	0.003	0.623	0.005
z2 3	3.62	0.191	0.238	0.007	0.285	0.177	0.002	0.573	0.003
z3 3	3.53	0.161	0.296	0.069	0.377	0.173	0.003	0.468	0.007
z4 3	3.46	0.167	0.349	0.056	0.307	0.138	0.006	0.486	0.005
z5 3	3.45	0.159	0.353	0.002	0.367	0.158	0.004	0.472	0.002
zt 3	3.54	0.184	0.291	0.006	0.351	0.165	0.004	0.534	0.002
z1 4	3.70	0.240	0.200	0.000	0.308	0.186	0.005	0.636	0.002
z2 4	3.56	0.198	0.273	0.008	0.349	0.168	0.002	0.591	0.005
z3 4	3.45	0.165	0.354	0.112	0.402	0.179	0.008	0.516	0.006
z4 4	3.40	0.152	0.399	0.162	0.332	0.161	0.004	0.464	0.004
z5 4	3.41	0.158	0.392	0.001	0.282	0.150	0.004	0.481	0.003
zt 4	3.48	0.174	0.329	0.001	0.243	0.159	0.003	0.532	0.001
z1 5	3.69	0.254	0.203	0.000	0.269	0.185	0.003	0.659	0.000
z2 5	3.59	0.213	0.258	0.023	0.262	0.166	0.002	0.614	0.002
z3 5	3.50	0.183	0.319	0.060	0.322	0.207	0.007	0.525	0.004
z4 5	3.43	0.167	0.368	0.078	0.318	0.170	0.008	0.490	0.004
z5 5	3.43	0.160	0.372	0.004	0.298	0.159	0.004	0.470	0.003
zt 5	3.49	0.179	0.325	0.001	0.333	0.157	0.003	0.507	0.003

ANNEX 4

Figure 5a-e. Plots of concentration of different elements in the concentrations obtained with the weathering experiment with acid solution. The largest deviation in each graph is indicated.

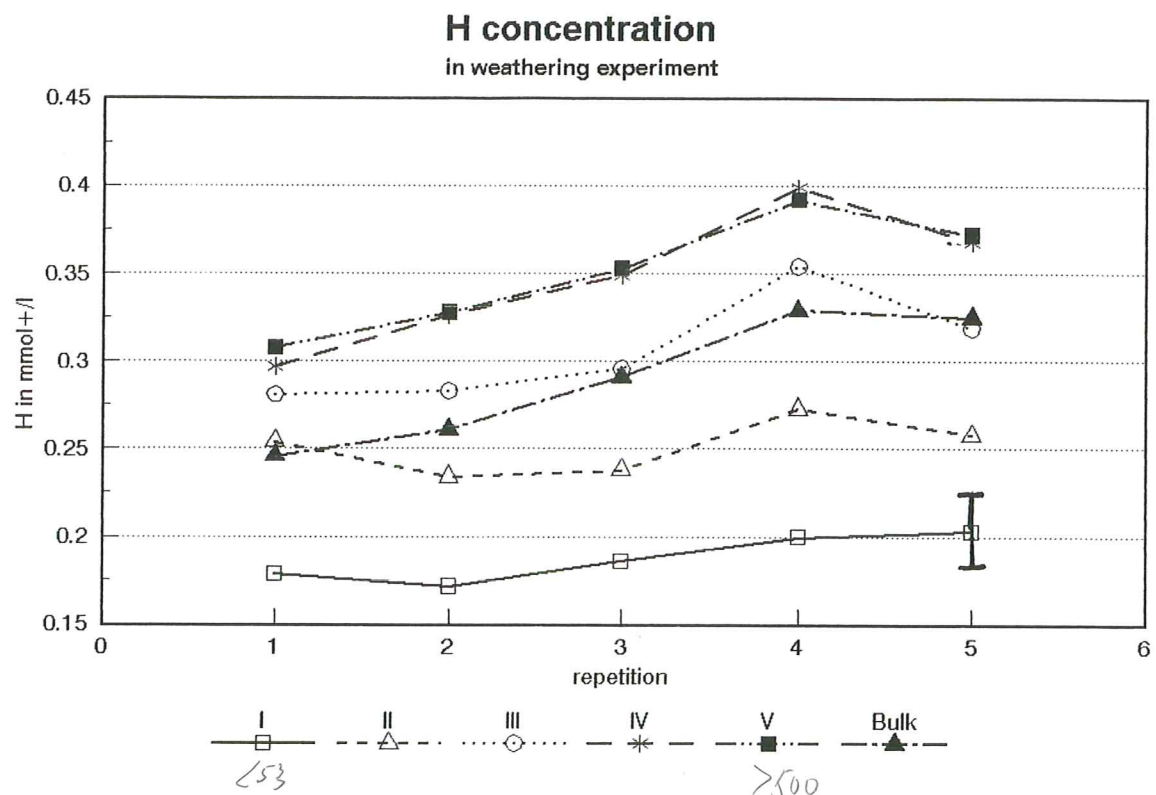


Figure 5a

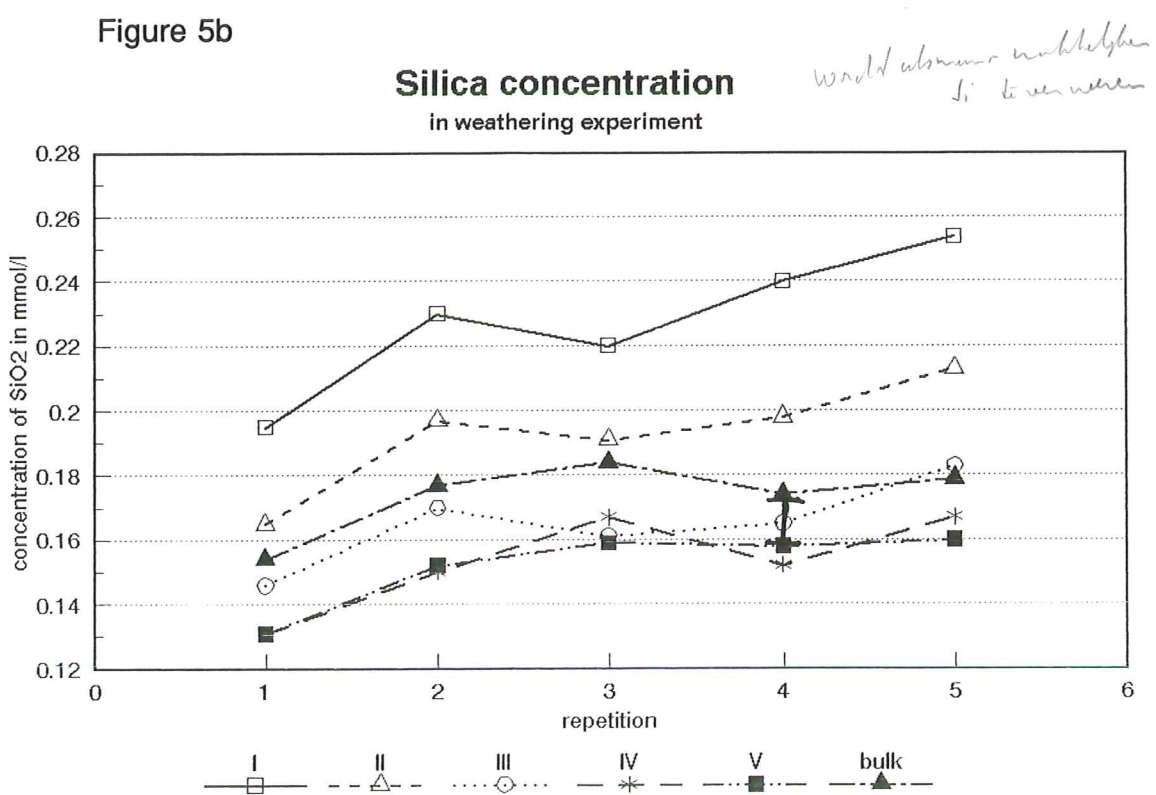


Figure 5b

ANNEX 4 (cont.)

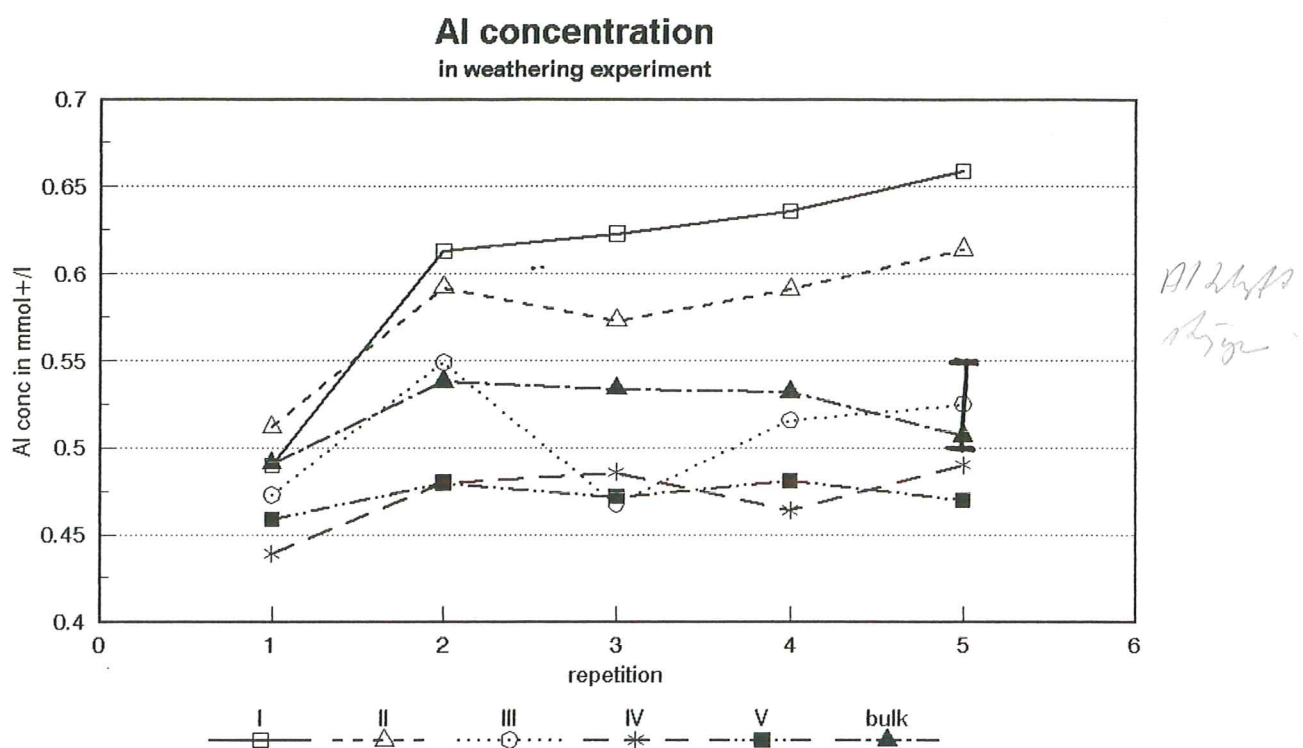
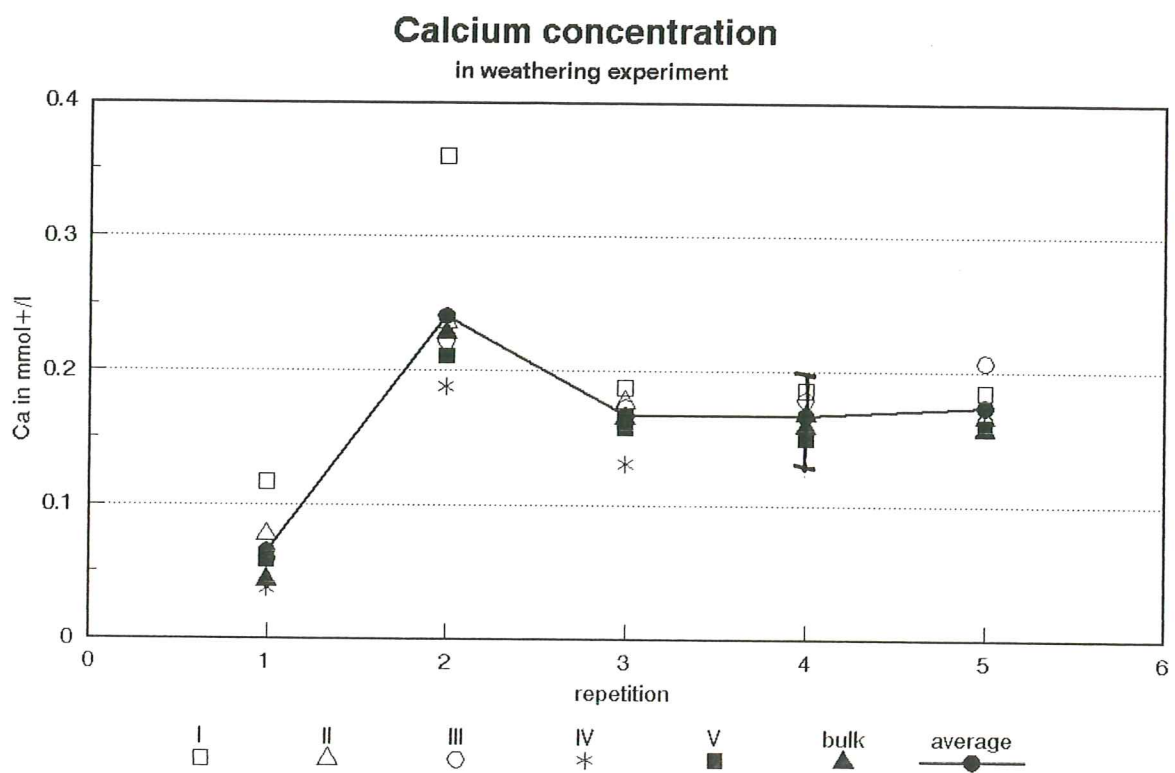


Figure 5c

Figure 5d



ANNEX 4 (cont.)

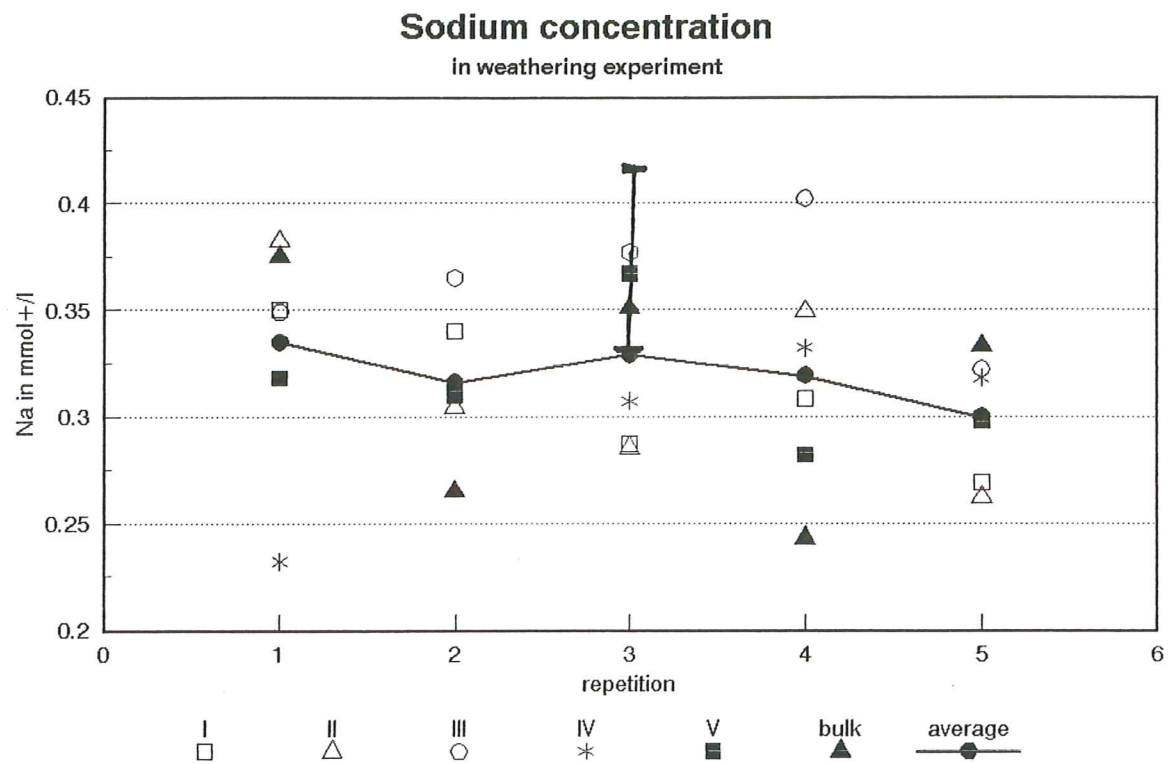


Figure 5e

ANNEX 5

Table 8. The chemical analysis of the solutions of the weathering experiment with water.

SAMPLE	pH	in mmol+/l (SiO ₂ in mmol/l)							
		SiO ₂	H	K	Na	Ca	Mg	Al	Fe
w1	5.81	0.071	0.002	0.001	0.250	0.124	0.001	0.003	0.004
w2	5.85	0.042	0.001	0.001	0.225	0.109	0.002	0.000	0.002
w3	5.82	0.034	0.002	0.007	0.243	0.112	0.002	0.000	0.003
w4	5.88	0.033	0.001	0.002	0.204	0.151	0.002	0.000	0.002
w5	5.88	0.034	0.001	0.008	0.155	0.101	0.003	0.000	0.002
wt	5.82	0.055	0.002	0.002	0.157	0.101	0.002	0.000	0.002

ANNEX 6

Aluminum can form complexes with water:



(Bolt and Bruggenwert, 1976)

The mean pH of the weathering experiment with acid solution is 3.55 (st. dev. is 0.10). If we use this value in the equations, the following equilibria are found:

$$(AlOH^{2+})/(Al^{3+}) = 2.82 \times 10^{-9} \quad (5)$$

$$(Al(OH)_2^+)/(Al^{3+}) = 3.55 \times 10^{-7} \quad (6)$$

$$(Al(OH)_4^-)/(Al^{3+}) = 1.58 \times 10^{-10} \quad (7)$$

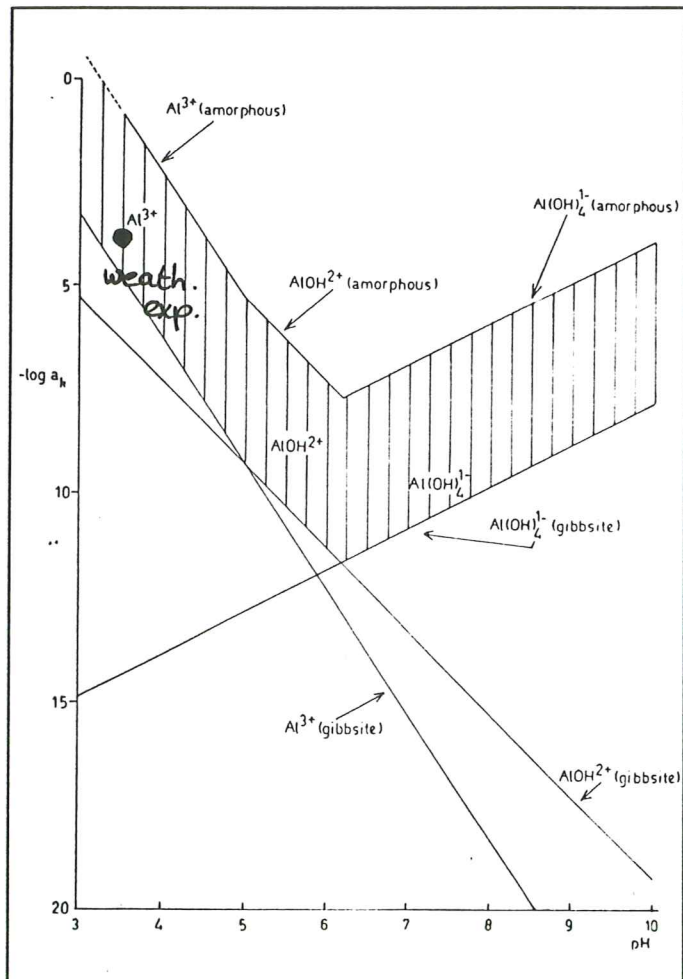
$$(Al_2(OH)_2^{4+})/(Al^{3+})^2 = 12.6 \quad (8)$$

The equilibria in equations 5, 6 en 7 can be neglected. The concentrations of the forms of Al in equation 8 can be calculated with the total Al concentration, which is the sum of both forms of Al. Al_{tot} is 0.525 mmol/l, which is 1.75×10^{-4} mmol/ml.

Calculation gives a concentration for $Al_2(OH)_2^{4+}$ which is practically zero, as a result the concentration of Al^{3+} is practically equal to the concentration of total Al, namely 1.75×10^{-4} mmol/ml. The activity coefficient of Al^{3+} is about 0.7 at this concentration (Bolt and Bruggenwert, 1976), which gives an activity for Al^{3+} of 1.23×10^{-4} .

The negative logarithm of this activity is 3.9. This value is plotted in the solubility diagram below with a pH of 3.55.

ANNEX 6 (cont.)



Solubility diagram of gibbsite and Al(OH)_3 (amorphous). The shaded area represents the possible values of aluminum solubility in soil systems.

From this diagram can be deducted that with the used concentrations gibbsite will not be formed, nor amorphous aluminum.